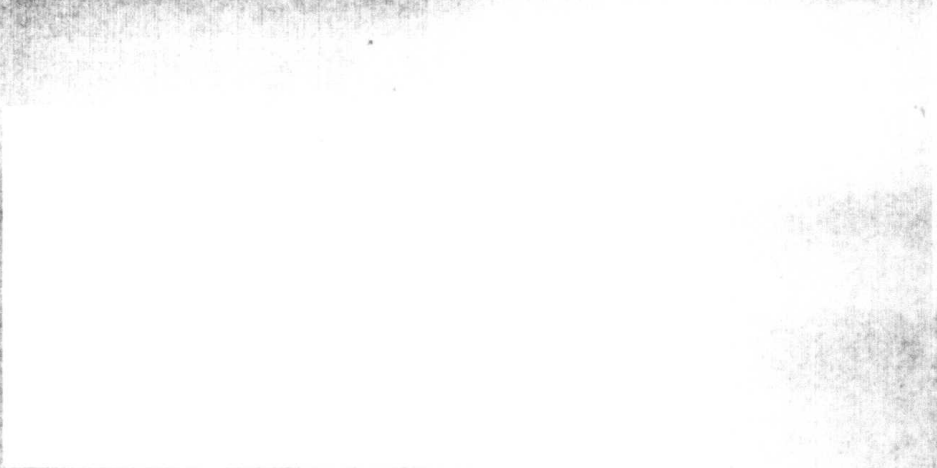


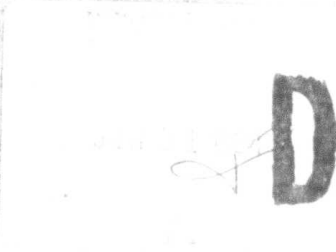
4

AD A142522



DTIC FILE COPY

Approved for public release
Distribution unlimited.



**ANALYSIS OF SHORT-PERIOD
P-CODA MEASUREMENTS FOR PRESUMED
UNDERGROUND NUCLEAR EXPLOSIONS IN EURASIA**

Douglas Baumgardt

13 April 1984

Sponsored By:

Advanced Research Projects Agency (DoD)
ARPA Order No. 4691
Monitored by AFOSR
Under Contract No. F49620-83-C-0041

JUN 21 1984

ENSCO, Inc.
Signal Analysis Systems Division
5400 Port Royal Road
Springfield, Virginia 22151

AIR FORCE OFFICE OF SCIENTIFIC RESEARCH (AFOSR)
NOTICE OF SPONSORSHIP OF TECHNICAL REPORT
This report is the property of the Air Force Office of Scientific Research (AFOSR) and is loaned to you. It and its contents are not to be distributed outside your organization.
Approved for Release by NSA on 05-08-2014 pursuant to E.O. 13526
DISTRIBUTION STATEMENT A
MATTHEW J. RENDLER
Chief, Technical Information Division

UNCLASSIFIED

SECURITY CLASSIFICATION OF THIS PAGE (When Data Entered)

| REPORT DOCUMENTATION PAGE | | READ INSTRUCTIONS BEFORE COMPLETING FORM |
|--|--|---|
| 1. REPORT NUMBER AFOSR-TR- 84-0478 | 2. GOVT ACCESSION NO. A142 522 | 3. RECIPIENT'S CATALOG NUMBER |
| 4. TITLE (and Subtitle) Analysis of Short-Period P-Coda Measurements for Presumed Explosions in Eurasia | | 5. TYPE OF REPORT & PERIOD COVERED Final Report 1 Jan. 1983-31 Jan. 1984 |
| 7. AUTHOR(s) Douglas R. Baumgardt | | 6. PERFORMING ORG. REPORT NUMBER SAS-TR-84-01 |
| 9. PERFORMING ORGANIZATION NAME AND ADDRESS ENSCO, Inc. 5400 Port Royal Road Springfield, Virginia 22151 | | 8. CONTRACT OR GRANT NUMBER(s) F49620-83-C-0041 |
| 11. CONTROLLING OFFICE NAME AND ADDRESS Air Force Office of Scientific Research Building 410 Bolling AFB, Washington, D.C. 20332 | | 10. PROGRAM ELEMENT, PROJECT, TASK AREA & WORK UNIT NUMBERS 61102F 4691-3A10 |
| 14. MONITORING AGENCY NAME & ADDRESS (if different from Controlling Office) | | 12. REPORT DATE 13 April 1984 |
| | | 13. NUMBER OF PAGES |
| | | 15. SECURITY CLASS. (of this report) UNCLASSIFIED |
| | | 15a. DECLASSIFICATION/DOWNGRADING SCHEDULE |
| 16. DISTRIBUTION STATEMENT (of this Report) Approved for public release; distribution unlimited. | | |
| 17. DISTRIBUTION STATEMENT (of the abstract entered in Block 20, if different from Report) | | |
| 18. SUPPLEMENTARY NOTES | | |
| 19. KEY WORDS (Continue on reverse side if necessary and identify by block number) | | |
| P Codas Semipalatinsk Explosions Azgir-Astrakhan Explosions | | NORSAR Data Body-Wave Scattering Lg Scattering |
| 20. ABSTRACT (Continue on reverse side if necessary and identify by block number) | | |
| We have investigated the characteristics of P-coda measurements at NORSAR for presumed underground nuclear explosions in the Soviet Union. For explosions in the Semipalatinsk region, we found that coda magnitudes, measured in the time domain in 5-second windows averaged over 50 seconds of P coda, varied by about 0.1 magnitude units across NORSAR as compared with about 0.2 to 0.3 units for P-wave magnitudes. Also, array-averaged estimates of coda magnitude varied more smoothly with time into the coda than single channel | | |

UNCLASSIFIED

SECURITY CLASSIFICATION OF THIS PAGE (When Data Entered)

estimates. This result indicates that local subarray scattering causes random perturbations in coda levels which are smoothed out by the averaging process. We find that NORSAR P-coda magnitudes, like the Lg measurements of Ringdal (1983), are more consistent with network averaged P-wave magnitudes than NORSAR single-channel magnitudes. There is some indication that Lg measurements may be slightly better than P-coda measurements in terms of reducing scatter and bias.

In our analysis of P-codas from seismic events north of the Caspian Sea, we find that codas of presumed explosions in the Astrakhan region are more intense and variable as a function of time into the coda than those for events near Azgir. We attribute these differences to lateral variations in geologic structure in the Pri-Caspian salt basin.

We have also investigated the question of how the P coda is generated; i.e., by surface-wave, or Lg, scattering or by body-wave scattering. The long-term codas, extending from first arrival P to the Lg arrival time, for Semipalatinsk events recorded at NORSAR pass through two distinct steps which we attribute to bursts of energy associated with the arrival of scattered and/or regional phases. The amplitudes of the phases in the first step, at about 200 seconds after P, correlate well with the amplitudes of Lg phases. However, the coda amplitudes between P and PP are poorly correlated with the Lg level. Thus, we argue that P-wave scattering in the source and receiver regions produces most of the coda energy between P and PP for Semipalatinsk events recorded at NORSAR. However, the coda between PP and Lg, or the Lg precursor coda, arises from Lg-to-P scattering and other regional phases, such as shear waves. The time between the energy burst in the coda and Lg is consistent with the burst being P waves produced by Lg-wave scattering in the vicinity of the southern Ural Mountains. Because of the close correlation between later Lg-precursor coda amplitudes and Lg and because the first flat part of the coda is about 0.1 to 0.2 magnitude units above the Lg level, coda magnitudes measured in this part of the coda may be more stable for yield estimation than either PP-precursor coda or Lg and Lg-coda measurements.



RE: Classified References, Distribution
Unlimited
No change per Mrs. Wert, AFOSR/XOTD

UNCLASSIFIED

SECURITY CLASSIFICATION OF THIS PAGE (When Data Entered)

ARPA Order No. 4691

Program Code 3A10

Effective Date of Contract: 1 January 1983

Original Contract Expiration Date: 31 December 1983

Extended Contract Expiration Date: 31 January 1984

Amount of Contract: \$120,419

Contract No. F49620-83-C-0041

Principal Investigator

Dr. Douglas R. Baumgardt
703/321-9000, Ext 406

Program Manager

Mr. William J. Best
202/767-4903

The views and conclusions contained in this document are those of the author and should not be interpreted as necessarily representing the official policies, either expressed or implied, of the Defense Advanced Research Projects Agency or the U. S. Government.

TABLE OF CONTENTS

| <u>SECTION</u> | <u>PAGE</u> |
|--|-------------|
| Abstract | ii |
| 1.0 Introduction | 1-1 |
| 2.0 P-Coda Magnitude Stability | 2-1 |
| 2.1 Introduction | 2-1 |
| 2.2 Origin of the Short-Period P-Coda | 2-1 |
| 2.3 Coda Measurement Methods | 2-6 |
| 2.4 Coda Magnitudes for Semipalatinsk Events | 2-9 |
| 2.5 Coda Measurements for Caspian Sea Events | 2-21 |
| 3.0 Origin of Codos from Eurasian Events | 3-1 |
| 3.1 Introduction | 3-1 |
| 3.2 Long-Codos from Eurasian Explosions | 3-1 |
| 3.3 PP-Precursor Coda Waves | 3-7 |
| 3.4 Lg Precursor Coda Waves and Lg Scattering | 3-15 |
| 3.5 Semipalatinsk Event Codos - Conclusions | 3-22 |
| 4.0 Conclusions and Recommendations | 4-1 |
| 4.1 Conclusions | 4-1 |
| 4.2 Recommended Future Research | 4-3 |
| Acknowledgements | iv |
| References | v |

ABSTRACT

We have investigated the characteristics of P-coda measurements at NORSAR for presumed underground nuclear explosions in the Soviet Union. For explosions in the Semipalatinsk region, we found that coda magnitudes, measured in the time domain in 5-second windows averaged over 50 seconds of P coda, varied by about 0.1 magnitude units across NORSAR as compared with about 0.2 to 0.3 units for P-wave magnitudes. Also, array-averaged estimates of coda magnitude varied more smoothly with time into the coda than single channel estimates. This result indicates that local subarray scattering causes random perturbations in coda levels which are smoothed out by the averaging process. We find that NORSAR P-coda magnitudes, like the Lg measurements of Ringdal (1983), are more consistent with network averaged P-wave magnitudes than NORSAR single-channel magnitudes. There is some indication that Lg measurements may be slightly better than P-coda measurements in terms of reducing scatter and bias.

In our analysis of P-codas from seismic events north of the Caspian Sea, we find that codas of presumed explosions in the Astrakhan region are more intense and variable as a function of time into the coda than those for events near Azgir. We attribute these differences to lateral variations in geologic structure in the Pri-Caspian salt basin.

We have also investigated the question of how the P coda is generated; i.e., by surface-wave, or Lg, scattering or by body-wave scattering. The long-term codas, extending from first arrival P to the Lg arrival time, for

Semipalatinsk events recorded at NORSAR pass through two distinct steps which we attribute to bursts of energy associated with the arrival of scattered and/or regional phases. The amplitudes of the phases in the first step, at about 200 seconds after P, correlate well with the amplitudes of Lg phases. However, the coda amplitudes between P and PP are poorly correlated with the Lg level. Thus, we argue that P-wave scattering in the source and receiver regions produces most of the coda energy between P and PP for Semipalatinsk events recorded at NORSAR. However, the coda between PP and Lg, or the Lg precursor coda, arises from Lg-to-P scattering and other regional phases, such as shear waves. The time between the energy burst in the coda and Lg is consistent with the burst being P waves produced by Lg-wave scattering in the vicinity of the southern Ural Mountains. Because of the close correlation between later Lg-precursor coda amplitudes and Lg and because the first flat part of the coda is about 0.1 to 0.2 magnitude units above the Lg level, coda magnitudes measured in this part of the coda may be more stable for yield estimation than either PP-precursor coda or Lg and Lg-coda measurements.

1.0 INTRODUCTION

Because of the increased emphasis during the past four to five years on improving the national technical means for monitoring the Threshold Test Ban Treaty (TTBT), DARPA-supported research has focused extensively on the problems of yield estimation with seismic data. Recent research results have shown that traditional methods of estimating yields using body-wave and surface-wave magnitudes suffer from a variety of sources of uncertainty and bias (Bache et al, 1981; Bache, 1982). Most current research efforts in yield estimation have concentrated on gaining a better understanding the nature and extent of yield-estimation errors and biases and developing methods for avoiding or correcting these problems. Many of these methods are currently being tested on a large seismic database and the results are being evaluated in order to determine what combination of magnitude measurement and correction methods will provide the most reliable estimates of yields of underground nuclear explosions (Murphy and Bennett, 1983).

Other recent studies have investigated the use of other alternative methods of estimating explosion yields, including P-coda magnitudes (Baumgardt, 1983; Gupta, 1983, Bullitt and Cormier, 1983), Lg magnitudes (Alexander, 1983, Nuttli, 1983a, b) and Lg-coda magnitudes (Ringdal, 1983). All these studies indicate that magnitude measurements made on the scattered and higher-mode phases which arrive in the short-period coda after initial P appear to provide more stable and unbiased estimates of explosion source size than conventional P wave magnitudes.

Of the two methods, Lg magnitudes have been studied far more extensively. Nuttli (1973) first introduced $m_b(Lg)$ formula for estimating the size of small events at regional distances, and this magnitude measurement has been used extensively since. It has been found that $m_b(Lg)$, measured at 1 second period, is free of the focusing-defocusing and aesthenospheric absorption biases which plague P-wave m_b estimates (Ringdal, 1983). Moreover, unlike 20-second M_s , $m_b(Lg)$ does not appear to be strongly affected by the nonisotropic, tectonic component often associated with explosions (Chen, 1981; Roundout Associates, 1981; Alexander, 1983). However, Lg amplitudes are affected by attenuation in the upper crust and crustal structure (Mitchell, 1983; Osagie and Mitchell, 1983) which may produce $m_b(Lg)$ network scatter on the order of 0.2 and 0.3 magnitude units. Therefore, if more than one station is to be used for yield estimation, corrections for regional Lg attenuation must be made.

Nuttli (1983a, b) corrects for Lg attenuation by estimating a frequency dependent coda Q using the method of Herrmann (1980) for each source-receiver pair. A path-dependent magnitude correction is then determined for the coda-Q estimate and applied to each of the source-receiver paths of interest for yield estimation. Although the original coda-Q methodology (Aki, 1969; Aki and Chouet, 1975) was developed for local earthquakes where the back-scattering model applies, Nuttli (1983a, b) has applied the method to regional distances as great as 1000 km. The applicability of the method to these large distances is apparently indicated by the low scatter in $m_b(Lg)$ versus log yield which Nuttli obtains for NTS explosions.

It has been known for some time that the scattered waves in codas of local earthquakes are remarkably stable as compared to the P wave (Aki, 1982). This observation prompted the recent studies of the possible use of teleseismic P-coda magnitudes for yield estimation. This method looks promising because coda magnitudes appear to be more stable, in terms of their amplitude fluctuations around networks and large-aperture seismic arrays, than short-period P-wave magnitudes. Thus, much of the current research effort has been directed toward the analysis of P-coda magnitudes.

The main focus of this study has been the analysis of P-phase and coda magnitudes recorded at NORSAR from explosions in the U. S. and USSR. The initial phase of this research, described by Baumgardt (1983), concentrated primarily on U. S. explosions recorded at NORSAR. Also, a limited amount of SDCS analog recordings of NTS explosions were analyzed. As a result of this initial study, we drew the following overall conclusions:

- o Coda magnitudes exhibit less variation around the NORSAR array (by 0.08-0.1 m_b units) and the SDCS network (by about 0.4 m_b units) than conventional P-phase magnitudes.
- o P-phase magnitude biases between the Pahute Mesa and Yucca Flat regions at NTS appear to be averaged out by coda magnitudes.
- o In general, magnitude-yield scatter for NORSAR and SDCS stations for coda and P-phase magnitudes are comparable for NTS explosion with yields above 100 kt.
- o For explosions at NTS with yields below 100 kt, lower signal-to-noise ratios in codas begin to

limit the reliability of coda magnitudes for yield estimation.

Our last two conclusions make the point that direct coda-magnitude measurements may not provide significant improvements over P-phase magnitudes in terms of reducing magnitude-log yield scatter, particularly for small-yield events. It appears that low signal-to-noise ratios in codas limit the utility of coda magnitudes for yield estimation to large events. However, for large events, P-coda magnitudes are definitely more stable than P-phase magnitudes and may be used as single-station approximations to network-averaged P-phase magnitudes.

This report describes the results of our continued analysis of P-coda magnitudes. We have primarily concentrated on the analysis of P codas from Russian events. We present the results of our stability analysis at NORSAR of P-coda magnitudes for presumed Soviet explosions in the Semipalatinsk and Azgir-Astrakhan regions. We also consider the relative importance of near-source and near-receiver scattering effects on P-codas for presumed Russian explosions. With regard to Semipalatinsk explosions, we compare the P-coda magnitudes with Lg and Lg coda magnitudes determined by Ringdal (1983) for NORSAR. We also consider possible mechanisms for the excitation of the P-coda at NORSAR from Semipalatinsk and the implications for source characterization and yield estimation.

2.0 P-CODA MAGNITUDE STABILITY

2.1 INTRODUCTION

In this Section, we discuss the relative stability of P-wave and P-coda magnitudes at NORSAR for presumed Soviet explosions. In Baumgardt (1983), it was shown that the scatter of coda magnitudes around NORSAR for NTS events is about 0.1 to 0.2 magnitude units less than that of P-wave magnitudes. In the first part of this section, we discuss the scattering mechanism as the cause of P-coda waves and why average coda-wave magnitude estimates have less spatial variance than P-wave magnitudes. We then present the results of a stability analysis of P and coda waves for several seismic events in the Semipalatinsk and Azgir-Astrakhan regions.

2.2 ORIGIN OF THE SHORT-PERIOD P-CODA

The term P-coda usually refers to seismic waves which follow the first-arrival P phase that are not commonly known phases, such as PcP, PP, pP, etc. Many of the coda waves from large earthquakes are believed to be produced by multiple shocks or "subearthquakes" occurring in an extended fault zone. However, coda waves from underground nuclear explosions cannot be explained as multiple shocks because explosions are usually point sources. Scattering is believed to be the main cause of short-period P-coda waves from explosions.

Figure 1 shows a number of examples of short-period P and coda from U.S. and presumed Soviet explosions recorded at NORSAR. This figure illustrates the great variety of characteristics of codas recorded at the same sensor for explosions in different parts of the world. The P and coda waves from the U. S. explosions are generally longer period than those from the Soviet explosions which may be a reflection of the longer propagation paths from the U. S. test sites to NORSAR than from the Soviet test sites to NORSAR. The Aleutian Islands explosion excited more energetic coda waves relative to P than the NTS explosions. Of the Soviet events, the Novaya Zemlya and Astrakhan explosions appear to generate more intense codas than the Semipalatinsk and Azgir explosions. The codas from the Azgir-Astrakhan region north of the Caspian Sea are complicated by multiple P-waves from the upper-mantle travel-time triplications.

The various types of scattering mechanisms which can contribute to the P coda are illustrated in Figure 2. The reciprocal surface-wave-to-P and P-to-surface-wave conversions from structural or topographic heterogeneities are represented in Figures 2(a) and 2(b). Greenfield (1971) has demonstrated the importance of the former mechanism for exciting the P codas for two events at Novaya Zemlya. Recently, Gupta et al (1984) has argued that the relative spectral characteristics of P and coda for NTS explosions indicate that fundamental-mode Rayleigh-to-P scattering in the source region is a primary cause of NTS-explosion codas observed at NORSAR. Key (1967) observed Rayleigh waves at 1 Hz produced by near-receiver scattering of P waves in a nearby lake valley. Figure 2(c) depicts asymmetric

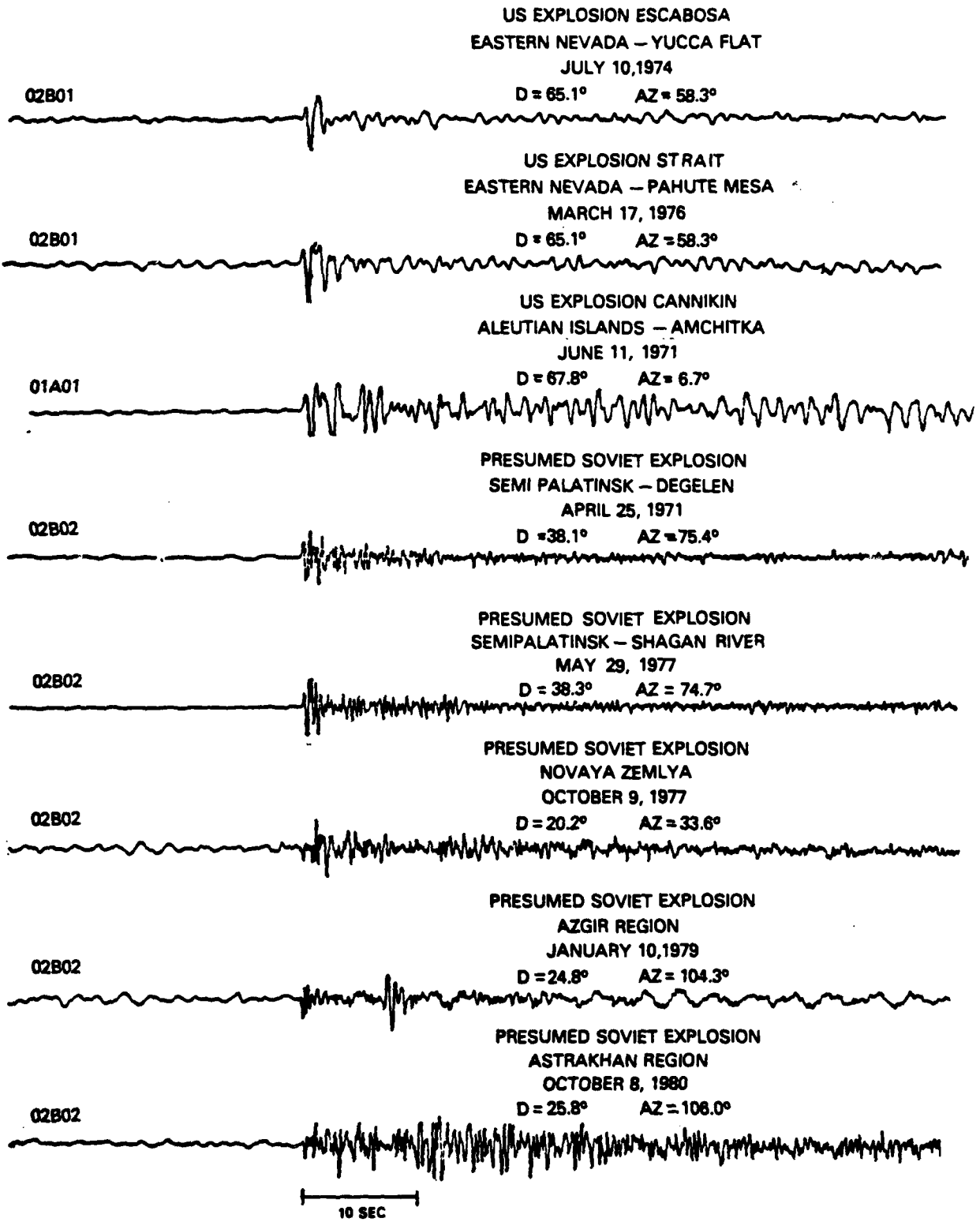


Figure 1. P and coda waves from U.S. and Russian explosions recorded at NORSAR

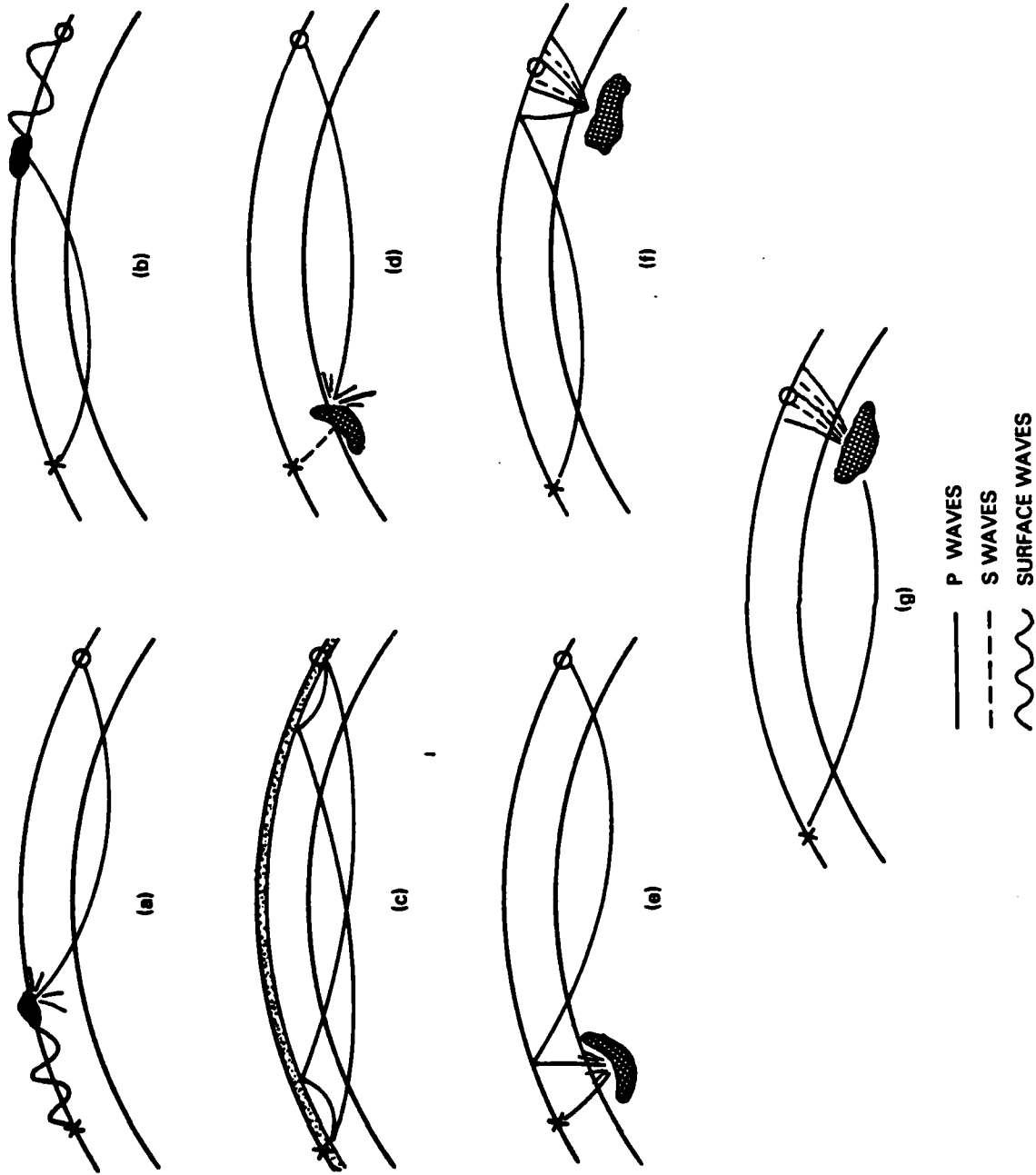


Figure 2. Schematic illustration of scattering mechanisms which can generate P-coda waves.

scattering from irregularities in the crust and upper mantle in the source and/or receiver regions, such as those observed by Wright and Muirhead (1969), King et al. (1973), and Cleary et al. (1975). Finally, localized irregularities beneath the source and/or receiver, such as igneous plutons or sharply folded layers, can act as secondary sources for body-wave scattering as shown in Figures 2(d) through 2(g).

As Figure 2 shows, source, path, and receiver scattering all contribute to the P coda in varying degrees depending on the relative amounts of heterogeneity in the different regions. Also, the relative contributions will differ for different test sites and source-receiver combinations. Thus, coda waves may be useful for characterizing different source, path, and receiver regions. For example, Gupta (1983) and Gupta et al (1984) have suggested that coda waves may be studied in order to extract near-source information. This may be accomplished by comparing P codas recorded at a common sensor for explosions at different test sites. However, the variations in P-coda characteristics apparent in Figure 1 for explosions at different test sites are not all due to differences in source characteristics; clearly, path contributions are also important. Therefore, in any discussion of the origin of P-coda waves, the reciprocal contributions from source and receiver regions and from along the path between source and receiver must be considered.

Current theories which attempt to explain the P coda usually represent coda waves as an ensemble of statistically scattered energy (e.g., Hudson, 1982). This may also offer

an explanation of the apparent stability of teleseismic P codas as compared with P waves. A P wave that arrives at a receiver has propagated along a single ray path. As shown schematically in Figure 3a, this ray path may be perturbed by local heterogeneities in the source and receiver regions which can induce substantial fluctuations in the P wave amplitude by focusing and defocusing. Ringdal (1981) and Ringdal et al (1983) have documented such ray-parameter dependent focusing-defocusing in the variability across NORSAR of the amplitudes of multiply refracted P waves in the upper mantle. The coda, on the other hand, can be thought of as a realization of the stochastic-scattering process which involves many scattered waves propagating along many ray paths (Figure 3b). Although any single ray path will experience the same focusing-defocusing effects as a single P wave, P-coda magnitude measurements made in time windows average over many such phases and thus, in effect, eliminate these random amplitude fluctuations and biases in the averaging. The same thing happens when averaging P-wave magnitudes across networks which explains why coda magnitudes are more consistent with network average P-wave magnitudes than single-station magnitudes.

2.3 CODA MEASUREMENT METHODS

In this study of coda magnitudes for Soviet events, we use the same measurement methods as those described in Baumgardt (1983). As shown in Figure 4, all measurements are referenced with respect to the P arrival time at a given NORSAR channel. Measurements are made in the noise in 10 adjacent 5 second windows ahead of the P-onset time and in the coda starting at the P-onset time or 5 seconds after the

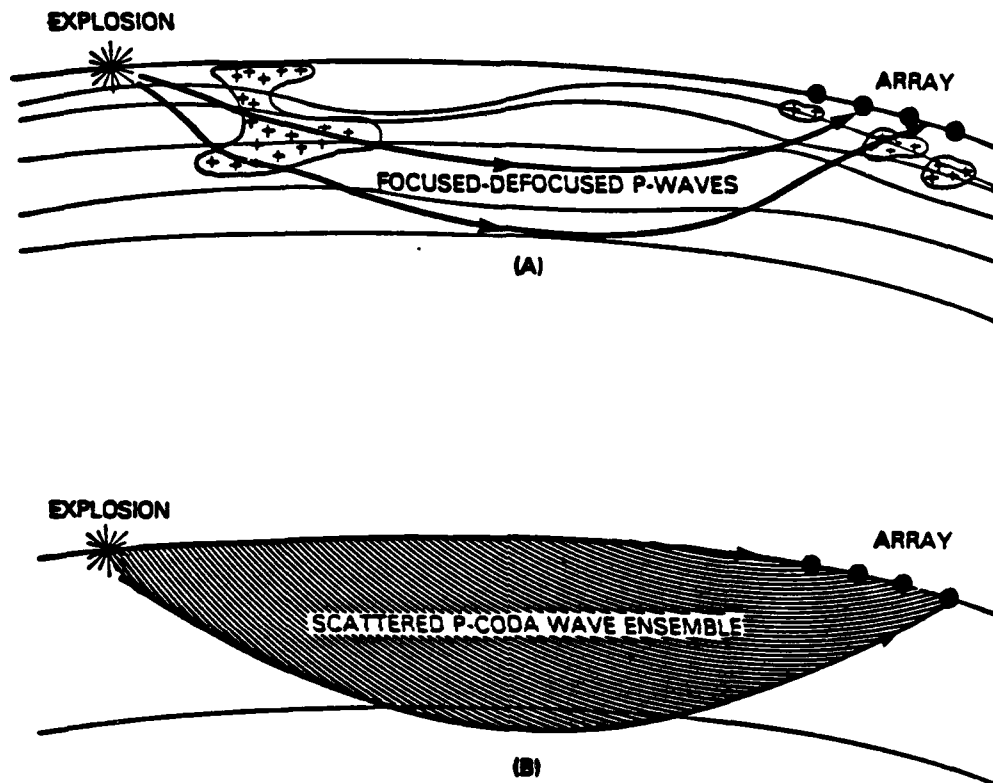


Figure 3. (a) Schematic illustration of focusing and defocusing of P waves.
 (b) Schematic illustration of scattered P coda waves as stochastic process.

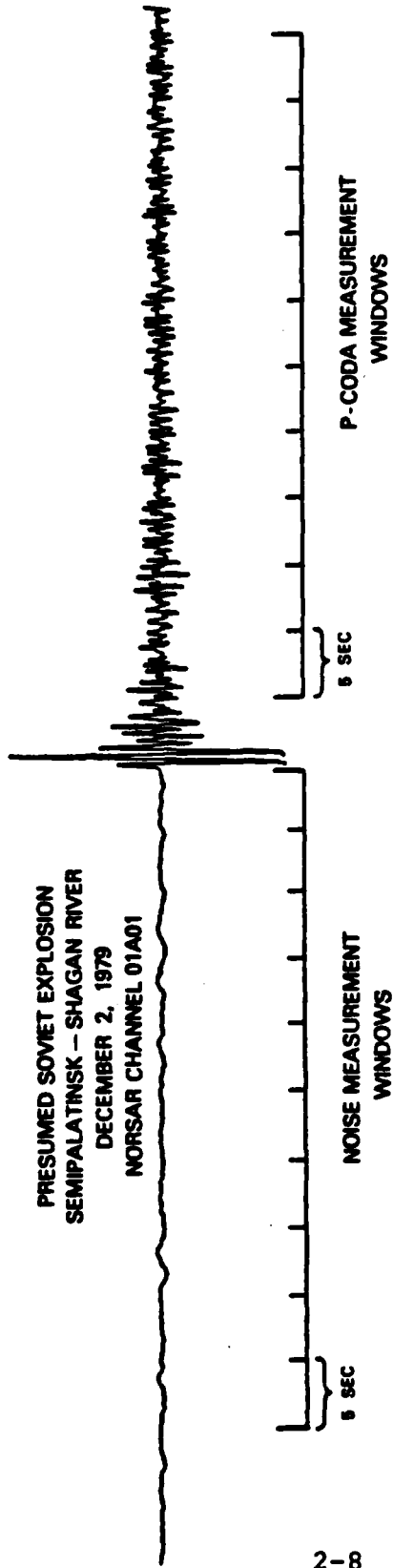


Figure 4. Time windows used for noise and P-coda magnitude measurements.

P onset time. For each 5 second window the logarithm of the RMS amplitude is computed. The noise and coda magnitude is then computed by averaging over the 10 log-RMS amplitude estimates in the 5 second windows.

In the earlier study (Baumgardt, 1983) the logarithm of the average rectified amplitude in each 5 second window was computed instead of the logarithm of the RMS amplitude. However, we have found the two magnitude estimates to have consistent relative trends although the log average rectified amplitude is larger than the log RMS amplitude by slightly less than a factor of two. In this study, we used log-RMS amplitude in order to compare P-coda magnitude estimates with the Lg-coda magnitudes of Ringdal (1983) who used a similar measurement method. As in the earlier study, no period normalization, instrument corrections, or distance correction, (i.e., B-factors) were applied to the coda-magnitude estimates. Ringdal (1983) also made no such corrections on Lg measurements.

2.4 CODA MAGNITUDES FOR SEMIPALATINSK EVENTS

P-coda magnitudes were computed for 23 events in the Semipalatinsk region of the Soviet Union. All but one of these events were also studied by Ringdal (1983). Each waveform was prefiltered with a 1.0 to 5.0 Hz, 6-pole, recursive bandpass filter prior to making noise and coda measurements.

Figure 5 shows a plot of the log-RMS amplitudes for several Semipalatinsk explosions, recorded at 03C01, for 45

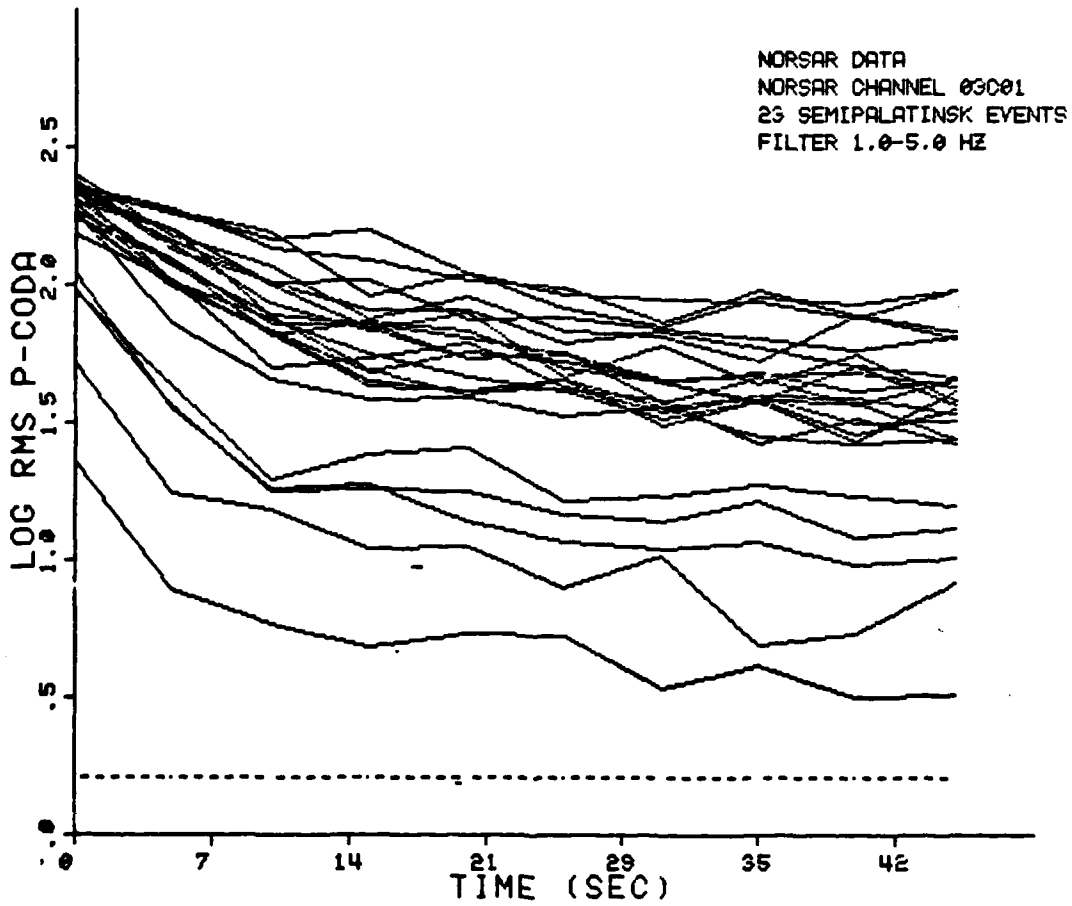


Figure 5. Log RMS amplitude levels in 10 adjacent 5 - second time windows on channel 03C01 starting at the P first arrival for 23 Semipalatinsk events. Dashed horizontal line is mean noise level before P onset.

seconds of P and coda. Figure 6 shows the same portion of coda but with the log-RMS amplitudes averaged over all available NORSAR subarray elements. It should be noted that for most of the large Shagan River explosions the P waves are clipped on most of the NORSAR sensors. Thus, the apparent convergence of the coda envelopes on the P wave at a value between 2.0 and 2.5 reflects the clipping of the P waves.

Comparing Figures 5 and 6 reveals that the array-average coda envelopes are smoother than the single-channel coda envelopes. Overall, the array-average coda envelopes in Figure 6 are roughly parallel although there is crossing and convergence of some of the coda trends. On the other hand, the single-channel coda trends in Figure 5 often criss-cross and are not always consistently decreasing with time. This result indicates that local subarray scattering effects cause perturbations in the coda levels at various times, as shown in Figure 5. Since these perturbations are random, they are smoothed out by averaging, as indicated in Figure 6.

Figure 7 shows the standard deviations within the 5 second windows of the log RMS coda levels. For most of the events in Figure 7 the standard deviations for the first 5 seconds (time 0 in Figure 7) are low because of the clipping effect. Most unclipped P-wave magnitudes have a variance of between 0.2 and 0.3 magnitude units across NORSAR. Figure 7 shows that the standard deviations for most of the codas range from 0.08 to 0.2 magnitude units with the average on the order of the average noise standard deviation of about 0.1 logarithmic units.

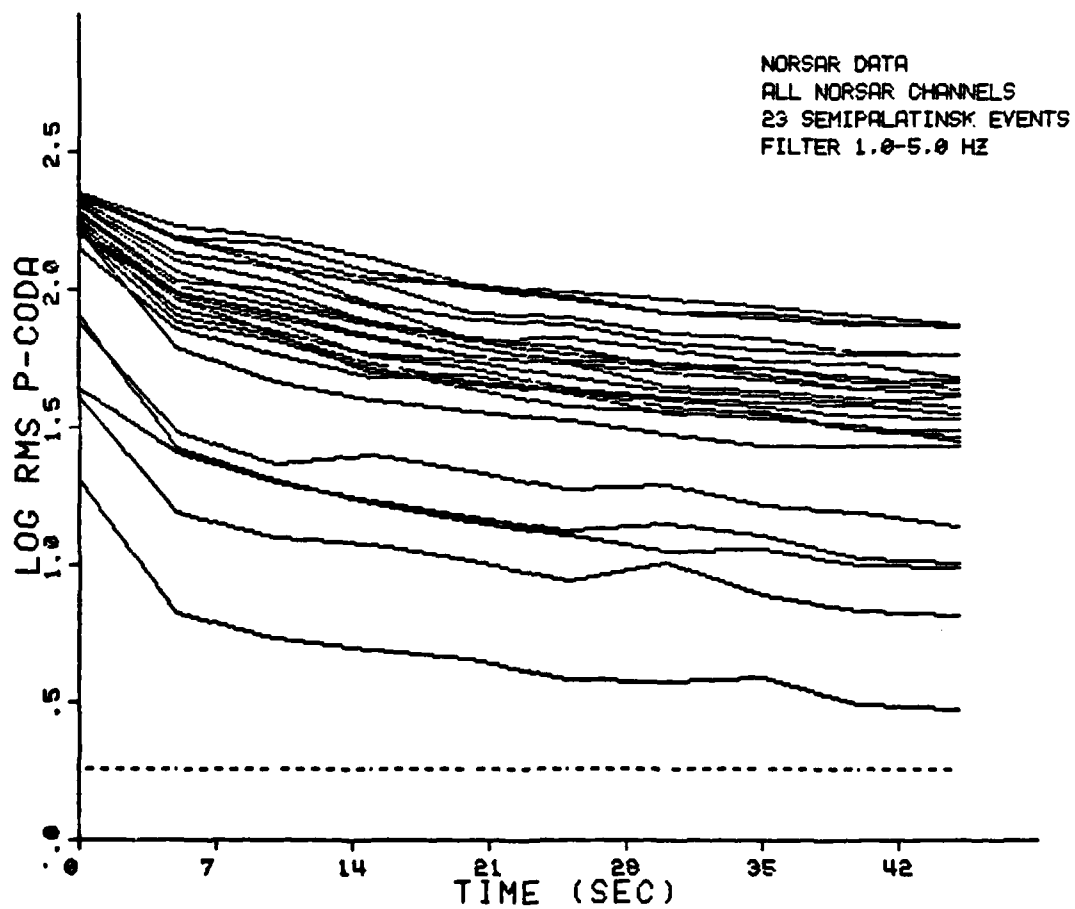


Figure 6. Same as Figure 5 except the P and log RMS coda levels are averaged over all usable NOR SAR subarray channels. Dashed horizontal line is mean noise level averaged over all channels and events.

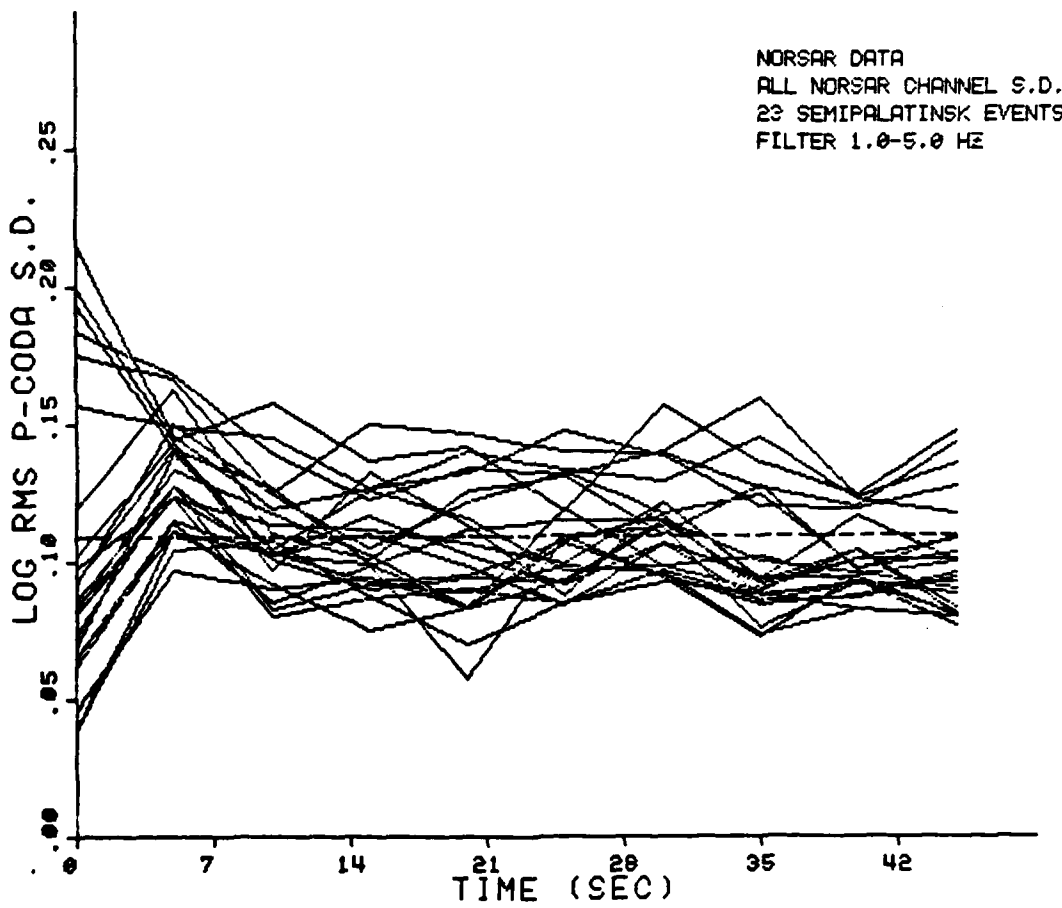


Figure 7. Standard deviation in the P and RMS coda levels.

In Table 1, the average single-channel and multichannel coda magnitudes are listed along with the network-averaged (NEIS and ISC) and NORSAR P-wave magnitudes. The coda magnitudes are averages of log-RMS amplitude made in 50 seconds of coda, starting 5 seconds after P, in the windows shown in Figure 4. The standard deviations, S, are averages of the standard deviations in each of the 5 second windows in the codas. Most of the average standard deviations lie between 0.09 to 0.11. Note that the highest standard deviations of 0.14 resulted for the low-magnitude Degelen explosions. Thus, the high standard deviations probably are a consequence of low signal-to-noise ratios in the codas.

Ringdal (1983) has pointed out that a comparison of the NORSAR magnitudes with NEIS or ISC network-averaged magnitudes reveals a bias between Shagan River and Degelen Mountain explosion magnitudes. Figure 8 shows the scatter plot of NORSAR versus NEIS magnitudes for the Semipalatinsk events used in this study. Except for the Degelen events, the database used in this study is the same as that of Ringdal (1983). Two Degelen events in the Ringdal (1983) database were not in ours whereas we included a small Degelen event which was not studied by Ringdal (1983). The bias of 0.4 to 0.7 logarithmic units between Degelen and Shagan NORSAR magnitudes is apparent in Figure 8 by comparing the NORSAR magnitudes for Degelen and Shagan events of comparable NEIS magnitude.

In Figure 9, the log-RMS coda magnitudes from Table 1 are plotted against the NEIS magnitudes. The log RMS magnitudes reduce scatter by a 0.07 unit standard deviation which compares with 0.1 unit reduction that Ringdal (1983)

TABLE 1

P-CODA MEASUREMENTS AT NORSAR FOR SEMIPALATINSK EVENTS

| <u>DATE</u> | <u>TEST SITE</u> | <u>(NEIS/ISC)</u> | m_D^{\dagger} <u>(NORSAR)</u> | $m_D^{\dagger\dagger}$ <u>(03C1)</u> | $M_C^{\dagger\dagger\dagger}$ <u>(All)</u> | <u>S</u> |
|-------------|------------------|-------------------|------------------------------------|---|---|----------|
| 05/29/77 | Shagan | 5.6/5.8 | 6.34 | 1.66 | 1.65 | 0.091 |
| 06/29/77 | Shagan | 5.3/5.3 | 5.84 | 1.14 | 1.13 | 0.104 |
| 08/17/77 | Degelen | 5.0/ | 5.40 | 0.65 | 0.61 | 0.129 |
| 09/05/77 | Shagan | 5.9/5.8 | 6.42 | 1.64 | 1.61 | 0.108 |
| 03/26/78 | Degelen | 5.5/5.6 | 5.74 | 1.21 | 1.15 | 0.140 |
| 04/22/78 | Degelen | 5.3/5.3 | 5.50 | 0.97 | 0.97 | 0.140 |
| 06/11/78 | Shagan | 5.9/5.9 | 6.38 | 1.76 | 1.75 | 0.101 |
| 07/05/78 | Shagan | 5.8/5.8 | 6.34 | 1.68 | 1.70 | 0.099 |
| 07/28/78 | Degelen | 5.7/5.7 | 5.74 | 1.30 | 1.28 | 0.140 |
| 09/15/78 | Shagan | 6.0/6.0 | 6.48 | 1.78 | 1.79 | 0.099 |
| 06/23/79 | Shagan | 6.3/6.2 | 6.68 | 2.00 | 1.98 | 0.091 |
| 07/07/79 | Shagan | 5.8/5.8 | 6.38 | 1.68 | 1.68 | 0.099 |
| 08/04/79 | Shagan | 6.1/6.1 | 6.72 | 1.99 | 1.98 | 0.101 |
| 10/28/79 | Shagan | 6.0/6.0 | 6.42 | 1.73 | 1.72 | 0.118 |
| 12/02/79 | Shagan | 6.0/6.0 | 6.52 | 1.89 | 1.91 | 0.086 |
| 06/29/80 | Shagan | 5.7/5.7 | | 1.61 | 1.64 | 0.134 |
| 10/12/80 | Shagan | 5.9/ | 6.20 | 1.64 | 1.61 | 0.119 |
| 12/14/80 | Shagan | 5.9/ | 6.39 | 1.76 | 1.77 | 0.107 |
| 12/27/80 | Shagan | 5.9/ | | 1.75 | 1.79 | 0.092 |
| 04/22/81 | Shagan | 5.9/ | 6.51 | 1.85 | 1.83 | 0.091 |
| 10/18/81 | Shagan | 6.01 | | 1.89 | 1.88 | 0.097 |
| 11/29/81 | Shagan | 5.6 | | 1.56 | 1.53 | 0.102 |
| 12/27/81 | Shagan | 6.2 | | 2.02 | 2.01 | 0.095 |

\dagger P-Magnitude made on 01A01 channel, from Ringdal (1983)

$\dagger\dagger$ Average of 10 estimates of logarithm of RMS amplitude made in 5 second windows starting 5 seconds after P-onset time on the 03C01 channel.

$\dagger\dagger\dagger$ Average over all available NORSAR channels of single-channel logarithm of RMS amplitude estimates.

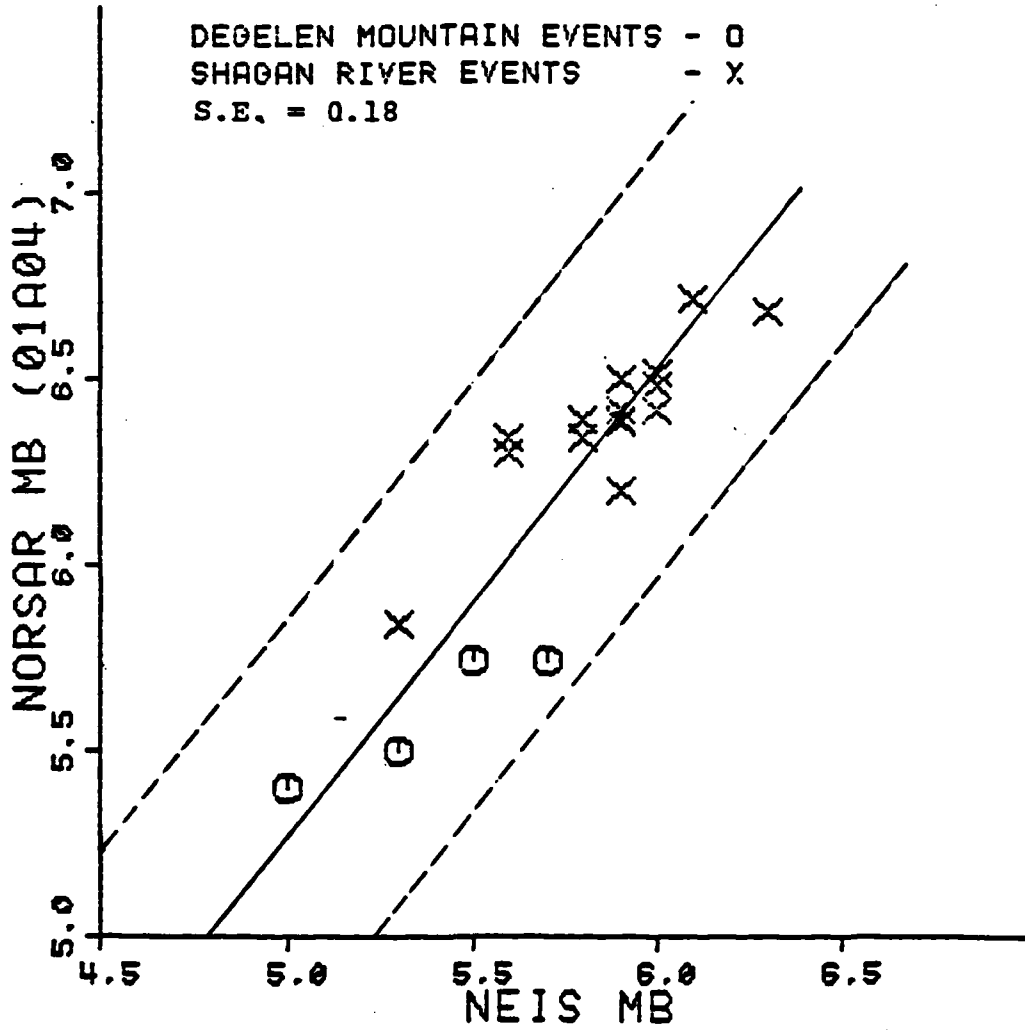


Figure 8. NORSAR magnitudes, measured on channel 01A04, plotted against NEIS magnitudes for Semipalatinsk events. Dashed lines represent plus and minus two standard deviations.

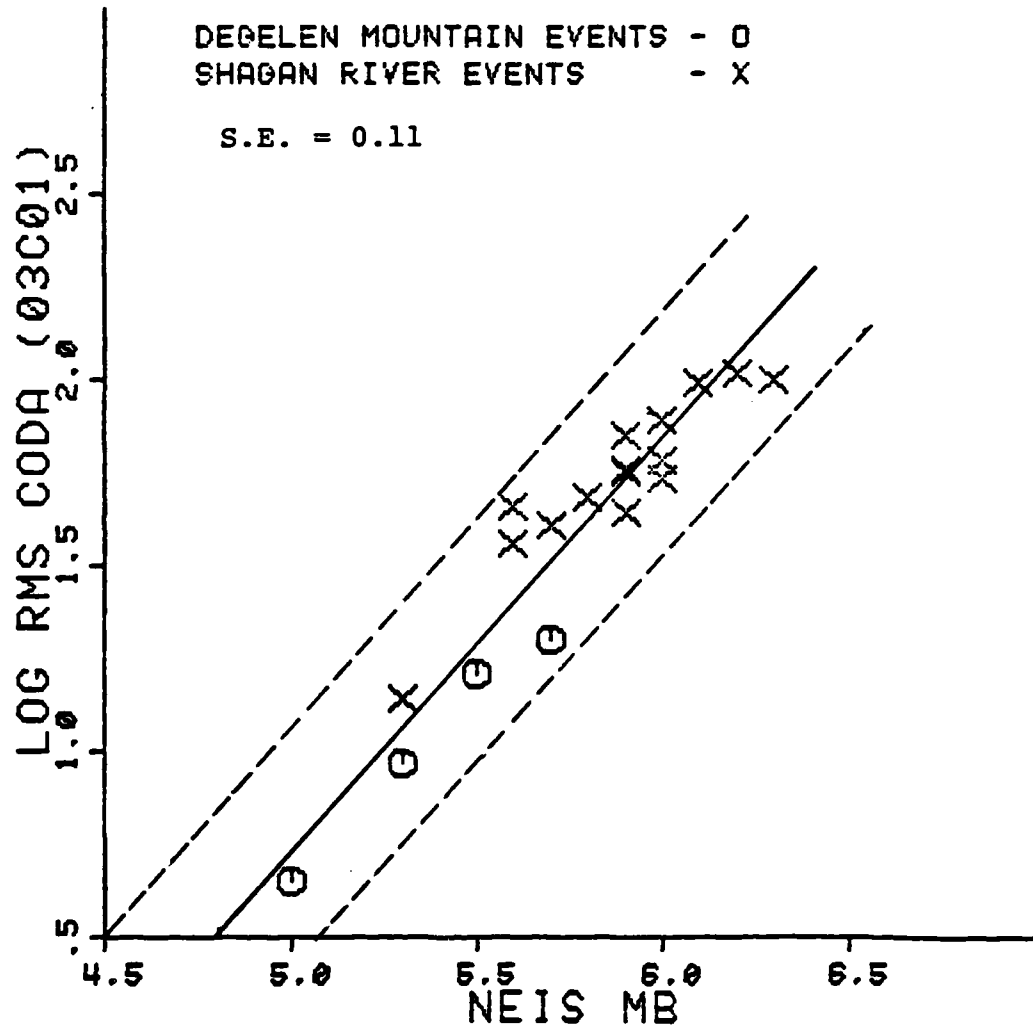


Figure 9. Single-channel (03C01) NORSAR subarray log RMS coda magnitude estimates plotted against NEIS magnitudes for Semipalantinsk events. Dashed lines represent plus and minus two standard deviations.

obtained for Lg-coda magnitudes. Also, Figure 9 indicates that the Degelen-Shagan River bias for coda magnitudes at NORSAR is about half of what it is for NORSAR P magnitudes or about 0.2 to 0.4 units. The bias for the Lg measurements of Ringdal (1983) may be even less than that for P coda measurements although this conclusion is problematic because of the limited amount of data.

Figure 10 shows a comparison of single-channel coda measurements with multichannel averages across all available NORSAR channels. Obviously, there is an excellent correspondence between the single channel and array-averaged coda measurements.

In Figure 11, the single channel coda measurements are compared with the single channel Lg-coda measurements of Ringdal (1983) for the same events. Figure 11 indicates that the P-coda and Lg measurements are approximately but not perfectly consistent. Although both sets of measurements were made on the same channel (03C01) for the same events, the measurement/methodologies used were not identical. Ringdal (1983) measured log-RMS amplitude in a single 2-minute window starting 40 seconds before the expected Lg arrival time. The P-coda measurements, described above, are averages of several measurements made in short (5 second) windows rather than a single measurement made in a long window. Thus, it is not clear if the scatter in Figure 8 is due to differences in measurement methodologies for P-coda and Lg or to a fundamental difference in the characteristics of P-coda, and Lg and Lg-coda phases.

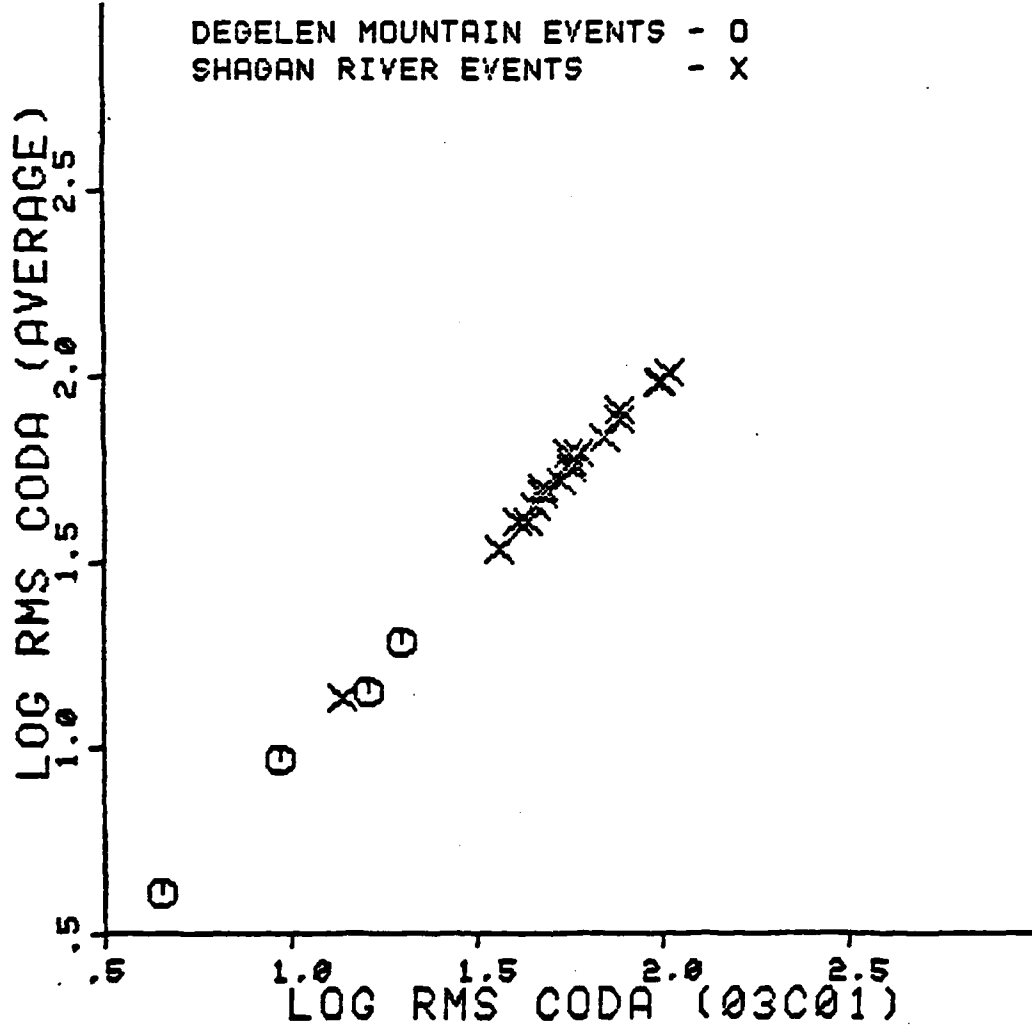


Figure 10. Comparison of coda measurements on a single channel with those averaged across all available NORSAR channels.

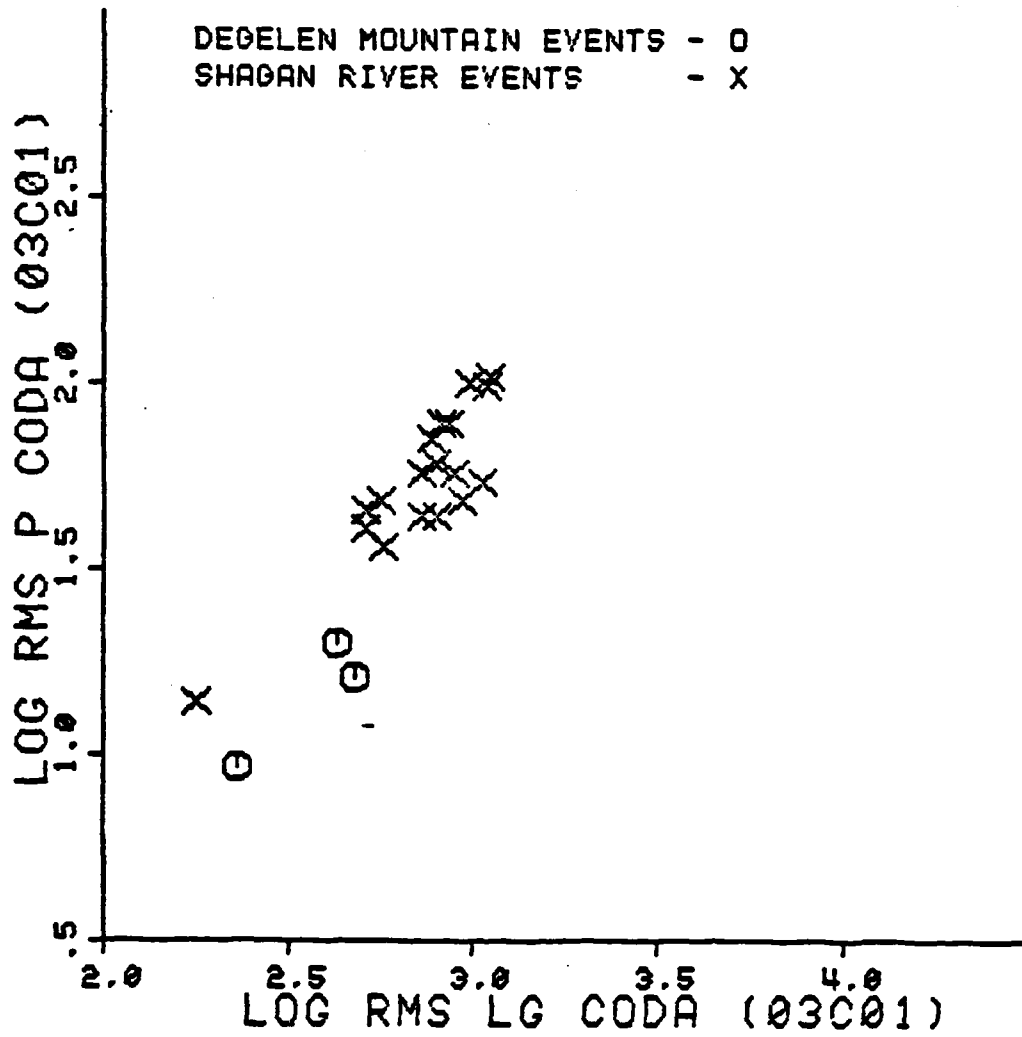


Figure 11. Comparison of single-channel P-coda measurements with single-channel Lq measurements of Ringdal (1938).

We also point out that the coda standard deviations in Table 1 are larger than those for Lg in Ringdal (1983); the Lg standard deviations are on the order of 0.05 to 0.08 logarithm units. The smaller Lg standard deviations may be a result of the fact that the Lg measurements were made in long 2 minute windows. As we demonstrated in Figure 5, coda measurements in short 5 second windows exhibit significant fluctuation in time although these variations are reduced by averaging over time and over several channels. Thus, the P-coda standard deviations would be lower if they were computed for longer time windows.

In conclusion, we find that NORSAR P-coda magnitudes, like the Lg measurements of Ringdal (1983), are more consistent with network averaged P-wave magnitudes than NORSAR single channel magnitudes. There is some indication that Lg measurements may be slightly better than P-coda measurements in terms of reducing scatter and bias. However, a more careful comparison of P-coda and Lg measurements, using the same measurement methodologies, must be made.

2.5 CODA MEASUREMENTS FOR CASPIAN SEA EVENTS

The two regions north of the Caspian Sea where presumed nuclear explosions have occurred are near Azgir, USSR, at about 48°N latitude, 48°E longitude and at Astrakhan, USSR, about 1 degree south of Azgir. These regions are part of a large salt basin, called the Pri-Caspian Depression (Piwinskii, 1981), and which contain some of the largest salt-dome accumulations in the world.

To date, there have been 15 presumed explosions in the Azgir region and 13 presumed explosions in the Astrakhan region. These events are apparently peaceful nuclear explosions (PNEs) whose purpose ostensibly is to generate standing cavities in the salt domes for the storing of natural gas (Nordyke, 1973; Kedrovskiy, 1975).

Examples of NORSAR recordings of an Azgir and Astrakhan event are shown at the bottom of Figure 1. Both traces exhibit significant complexity due to the presence of multiple P waves produced by the upper-mantle travel-time triplications. Two of these phases can be clearly observed in the case of the Azgir event though the signal-to-noise ratio is lower than in the Astrakhan trace. The Astrakhan event has apparently generated a more energetic coda than the Azgir event which partially obscures the upper-mantle P phases. The greater complexity of Astrakhan-event codas compared with Azgir-event codas may reflect a greater degree of near-source geological complexity in the Astrakhan region than in the Azgir region.

Figure 12 shows the RMS P and coda envelopes for nine Azgir events recorded at the 01A01 subarray element at NORSAR. The large seismic events at Azgir (above $m_b = 5.2$) produce clipped seismograms at most of the NORSAR channels except for channel 01A01, which has been specifically attenuated in order to avoid clipping. The 2.2 to 4.4 Hz bandpass filter was applied in order to enhance the first-arrival P phase (Ringdal et al, 1983). It is evident in Figure 12 that although the coda levels from these events

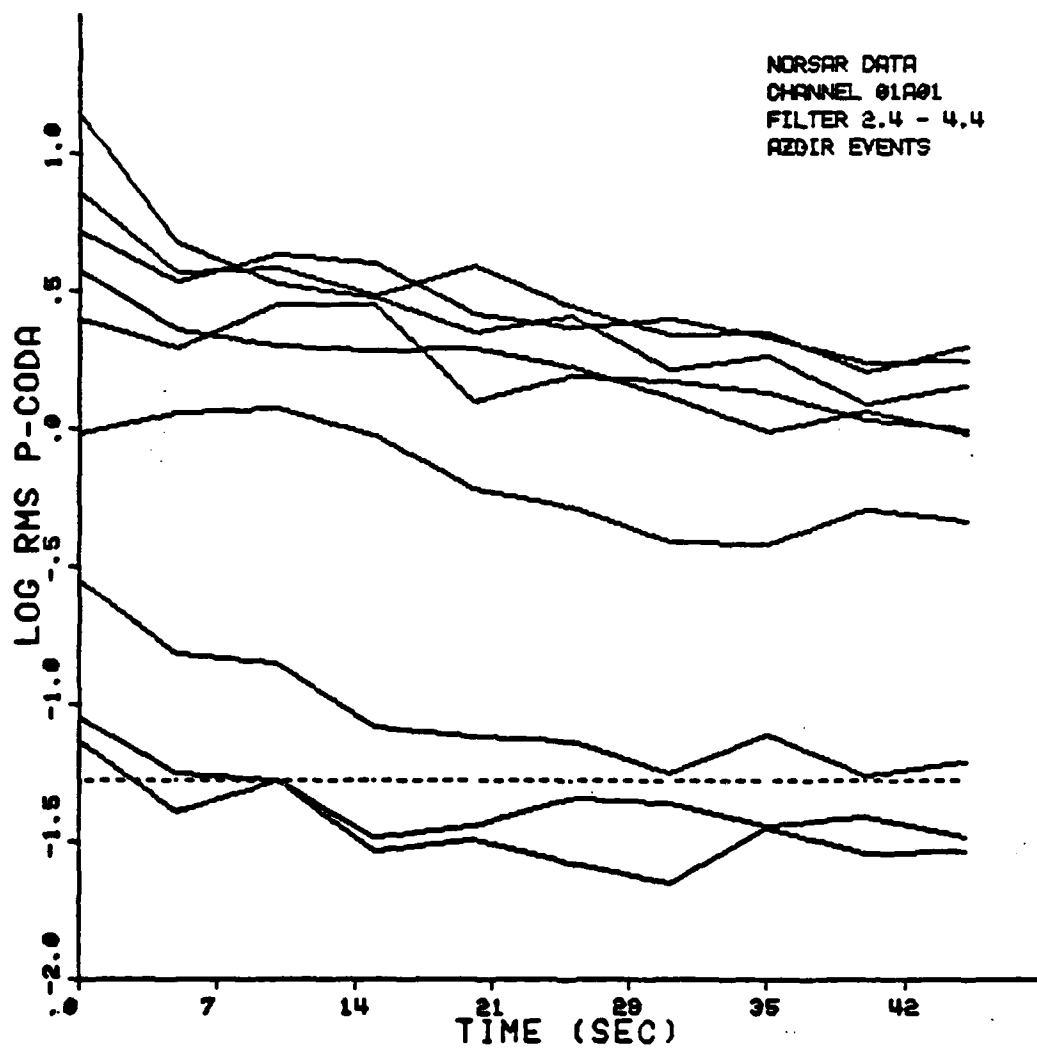


Figure 12. Log RMS amplitude levels in 10 adjacent 5 - second time windows in channel 01A01 starting at the P first arrival for 9 Azdir events. Dashed horizontal line is mean noise level before P onset.

drop approximately monotonically with time, there is a great deal of variability in amplitude levels at different times in the coda. Also, because of the signal attenuation on the 01A01 recordings, the smallest event codas fall quickly below the noise level. These small events have body-wave magnitudes well below 5.0, and the low signal-to-noise ratios on the 01A01 channel would render coda measurements on this channel useless for source characterization of small events at Azgir.

Figures 13 and 14 show plots of the log-RMS amplitude envelopes for the 5 smallest Azgir events recorded on the NORSAR channel 02B02. These are the only events which were not clipped on channels other than 01A01. The 1.2 to 3.2 Hz filter was applied in Figure 13 in order to enhance the second arrival P at about 6 seconds after P whereas the 2.4 to 4.4 Hz filter was applied in order to enhance the first arrival P in Figure 14. Ringdal (1981) and Ringdal et al (1983) has shown that the best signal-to-noise ratios at NORSAR for these two phases can be attained at the 02B subarray with these filters. Clearly, the coda levels in Figures 13 and 14 for the smallest events at Azgir are above the noise level although the 2.4-4.4 Hz filtered data appear to have higher signal-to-noise ratios in the codas than the 1.2 to 3.2 Hz data. The enhanced second arrival P phase at about 6 seconds after P can be seen in Figure 13.

Figures 15 and 16 show the array averaged log-RMS amplitude levels for the 5 events computed over all unclipped channels except 01A01. As in the case of the Semipalatinsk data discussed earlier, the array-averaged coda amplitudes for the different events are more parallel

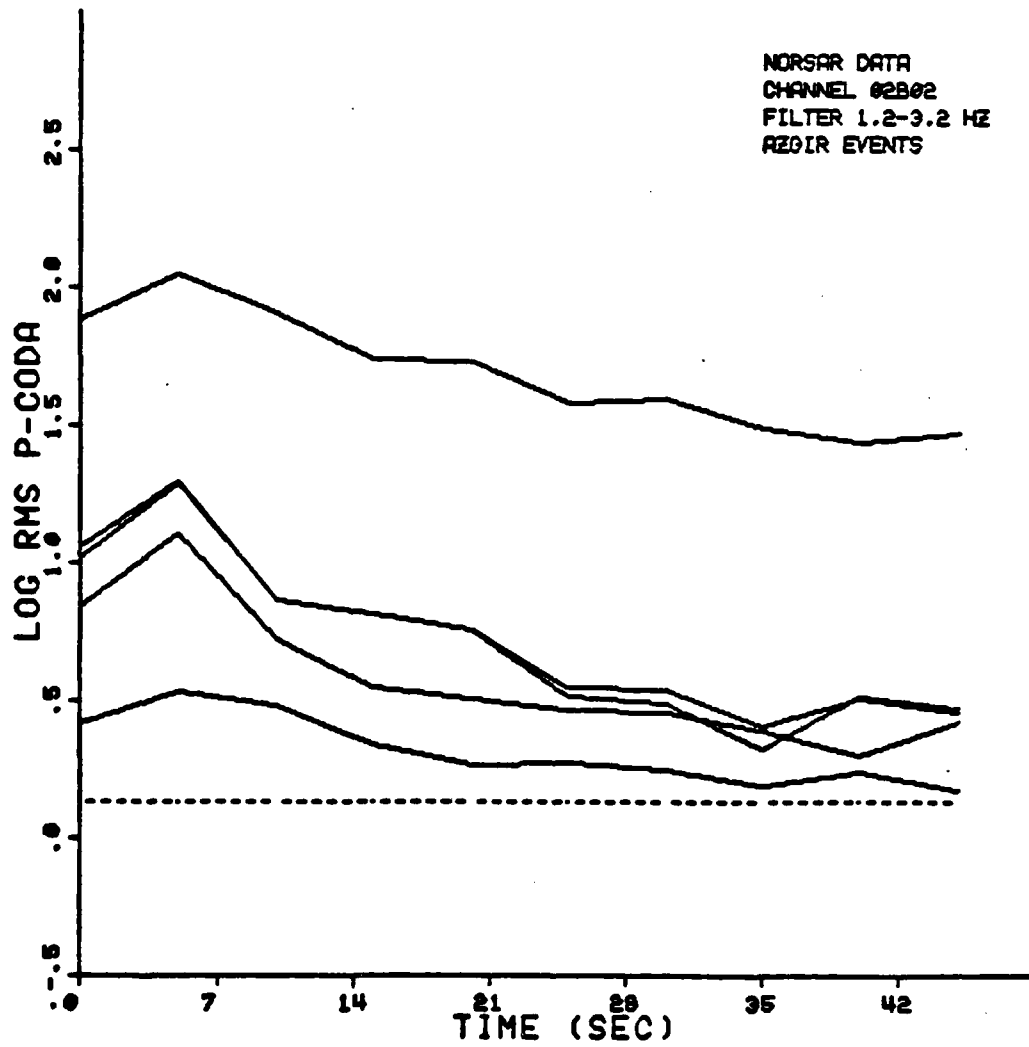


Figure 13. Log RMS amplitude envelopes for the 5 unclipped Azgir events at the NORSAR 02B02 subarray element. The 1.2 to 3.2 Hz filter applied to enhance second arrival P-phase at about 6 seconds.

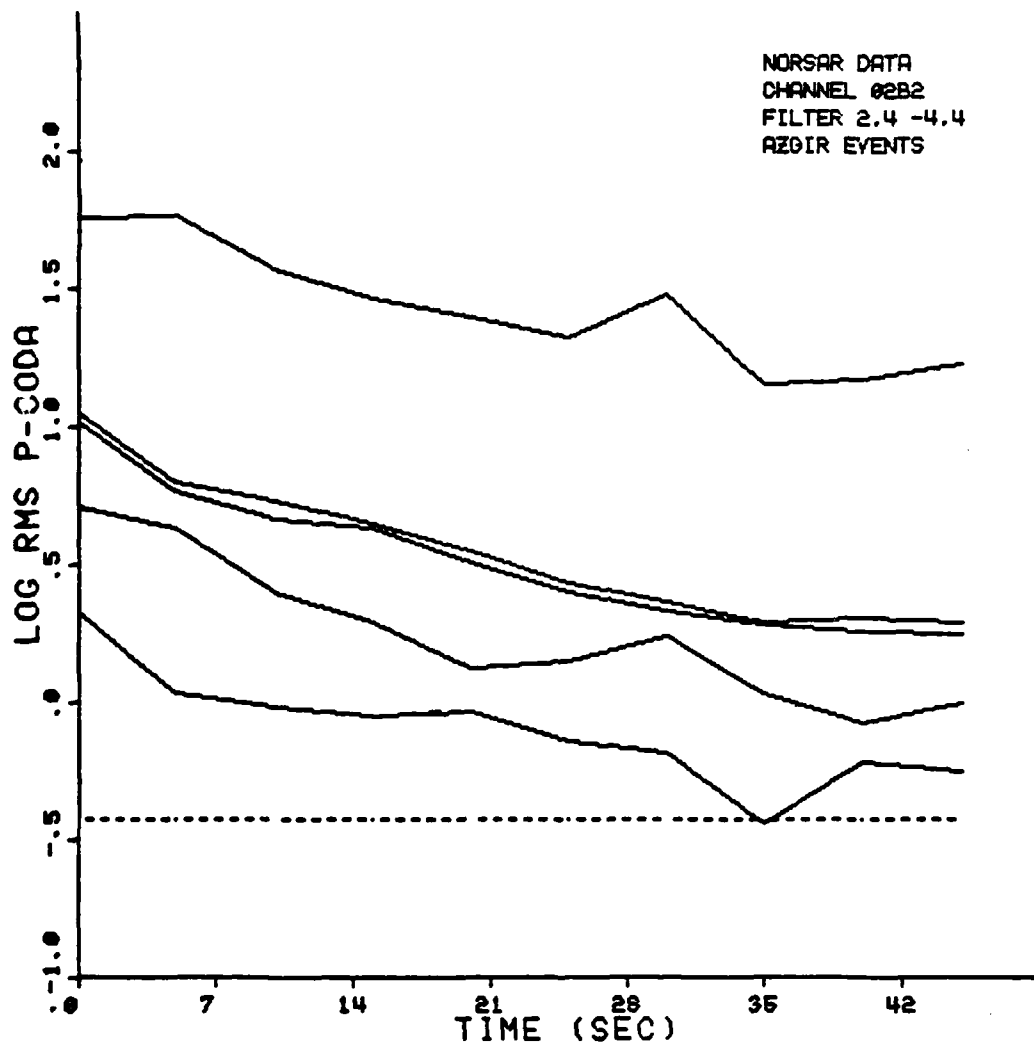


Figure 14. Same as Figure 13 except for the 2.4 to 4.4 Hz filter applied to enhance first arrival P.

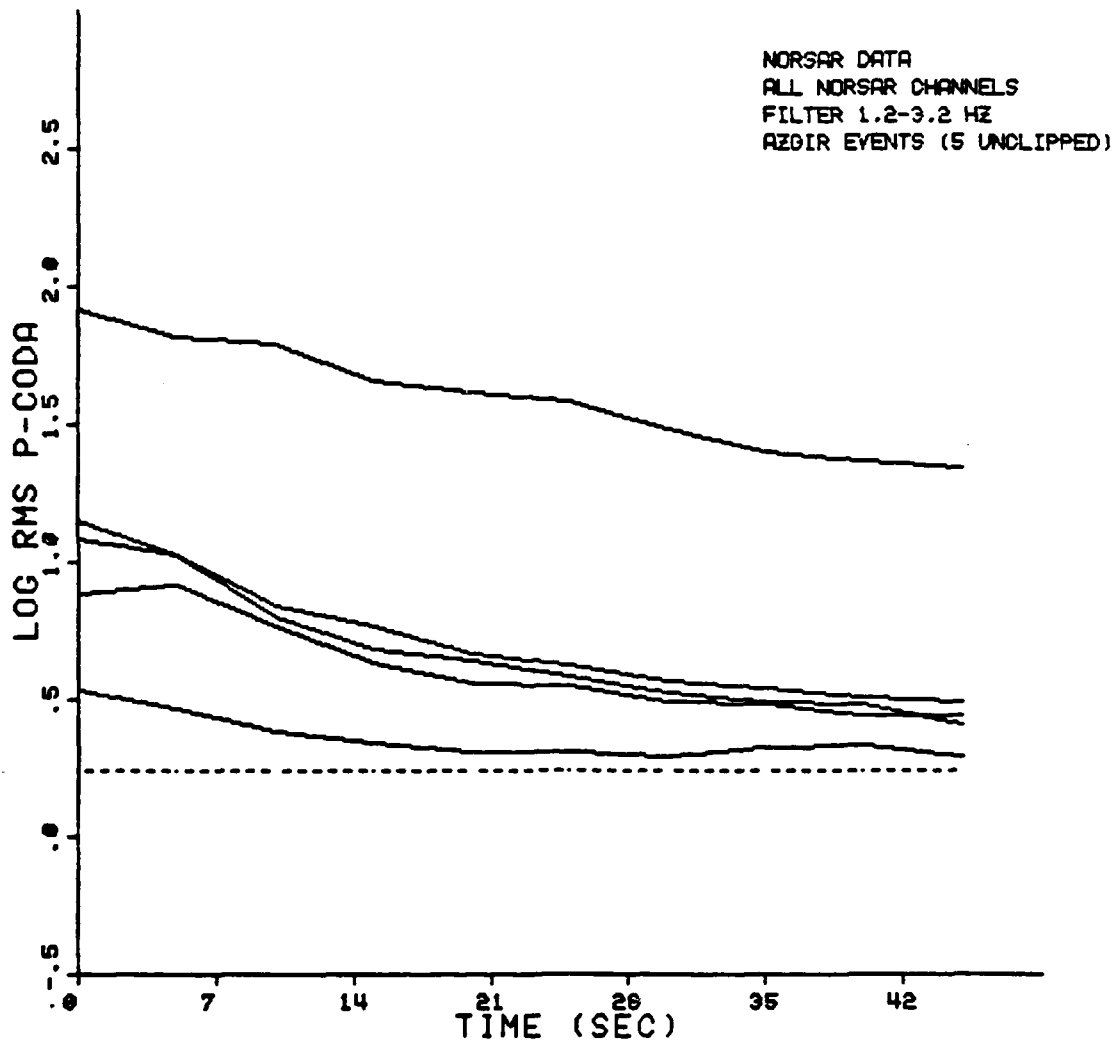


Figure 15. Log RMS amplitude envelopes averaged over all unclipped NOR SAR channels. Horizontal dashed line is mean noise before P averaged over all events and channels. 1.2 - 3.2 Hz filters applied to enhance second arrival P.

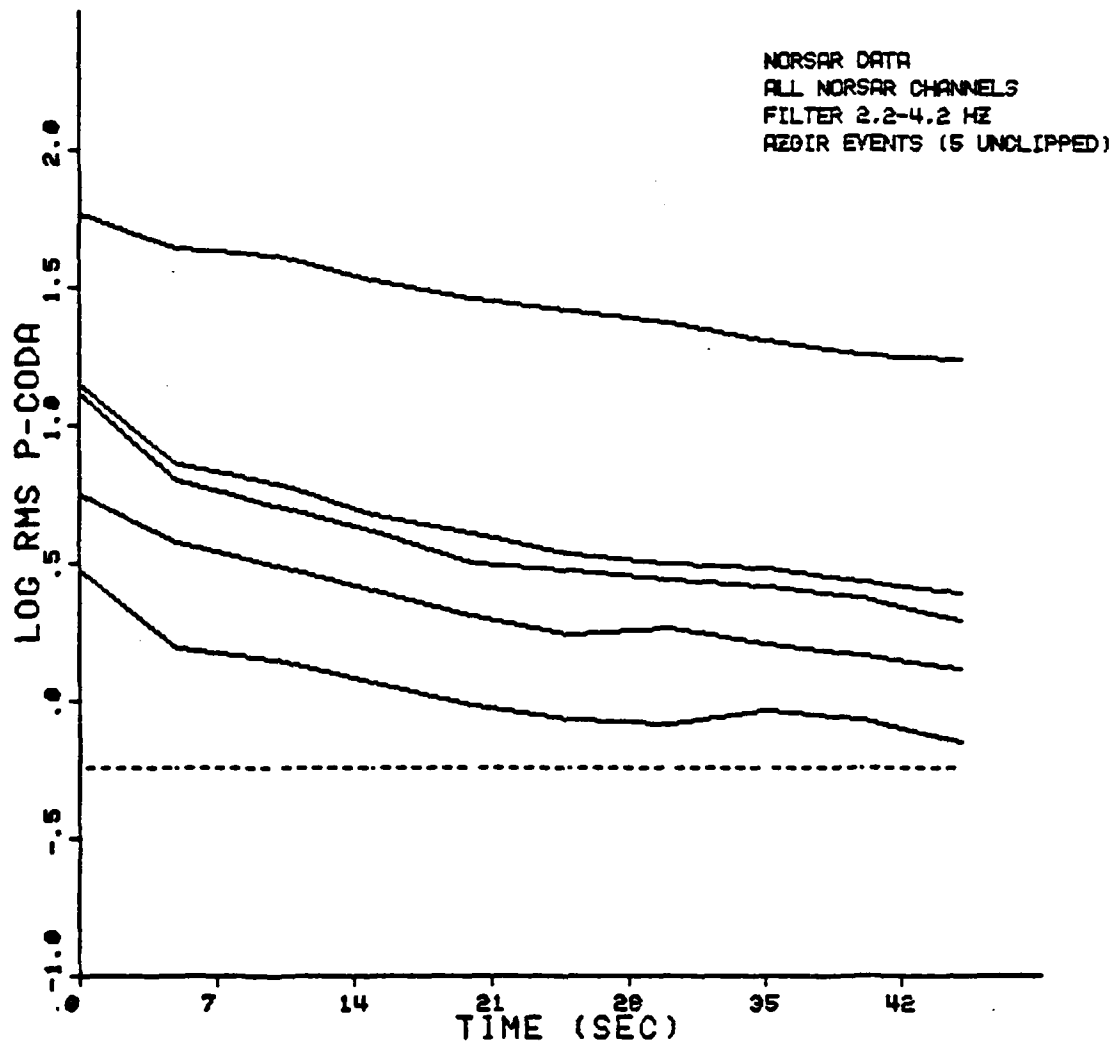


Figure 16. Same as in Figure 15 except that 2.2 - 4.2 Hz filter has been applied to enhance first-arrival P.

and decay more smoothly with time than the single channel codas. The standard deviations in the log-RMS amplitude levels in the two filtered bands are plotted in Figures 17 and 18. Notice the sharply increased standard deviation at the arrival time of the second-arrival P at about 6 seconds after P. Because the slowness of the second arrival P phase is greater by more than 1 sec/deg than the first arrival P phase (Ringdal, 1981; Ringdal et al, 1983) and because the standard deviations are computed from the traces lined up in time on the first arrival P, the higher standard deviation is expected for the second phase since it is misaligned. The first-arrival P and most of the coda has lower standard deviation comparable to the background noise. However, the first arrival P and all of the coda is below the noise level in the 2.2-4.2 Hz band as shown in Figure 18. Moreover, the mean noise standard deviation across NORSAR is higher in the 2.2 to 4.2 Hz band by about 0.05 logarithmic units than in the 1.2 to 3.2 Hz band. The reason why the coda standard deviation is lower than the noise standard deviation in the 2.2 to 4.2 Hz band in Figure 18, even though signal and noise RMS amplitude standard deviations are additive, is that the standard deviation in log RMS amplitudes in signal and noise are being compared. Since the log-RMS noise levels are less than zero and the signal RMS amplitudes are well above zero, the standard deviations in log-RMS noise levels will be greater than those for the signal even if the standard deviations in the RMS amplitudes without logs in signal and noise may be comparable.

Figures 19 and 20 show the single channel (03C01) and array-averaged envelopes for 12 Astrakhan events. All these events have nearly the same NEIS magnitudes of about 5.2 to

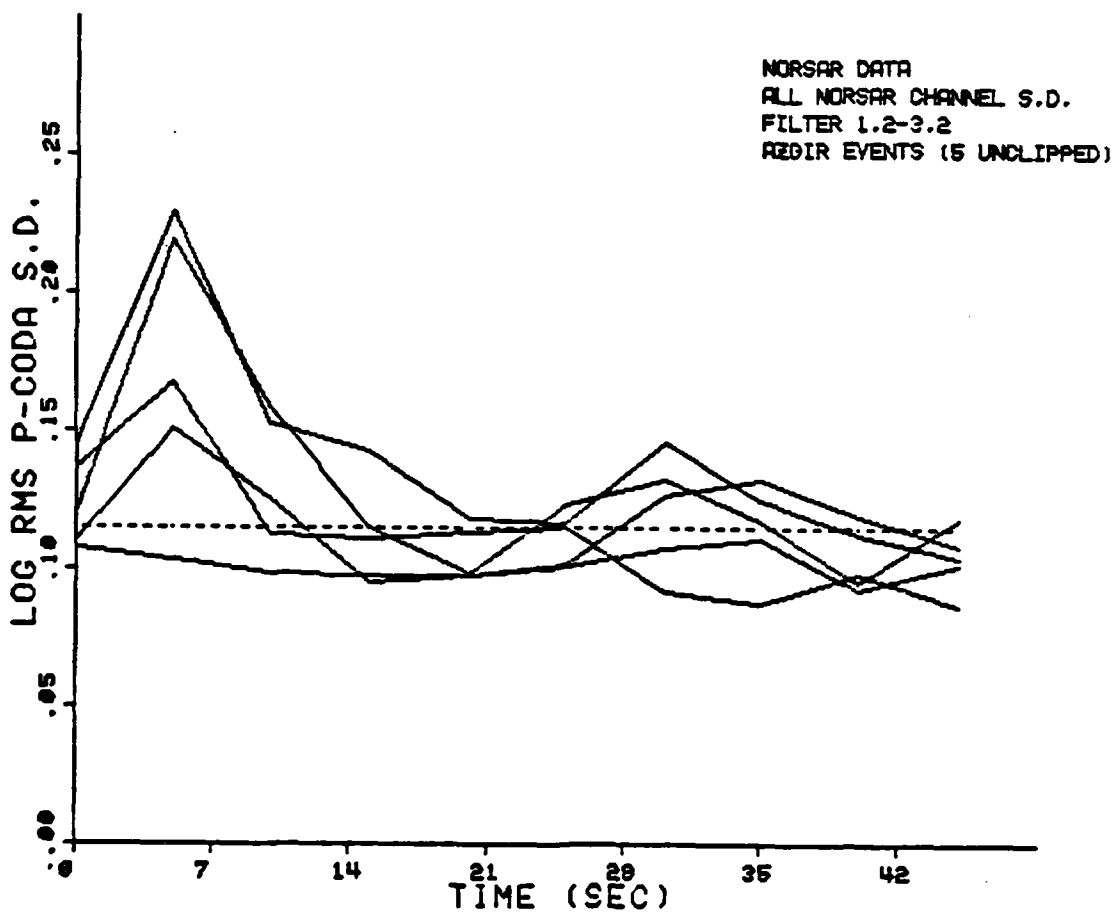


Figure 17. Standard deviation in RMS amplitude levels across all unclipped NORSAR channels.

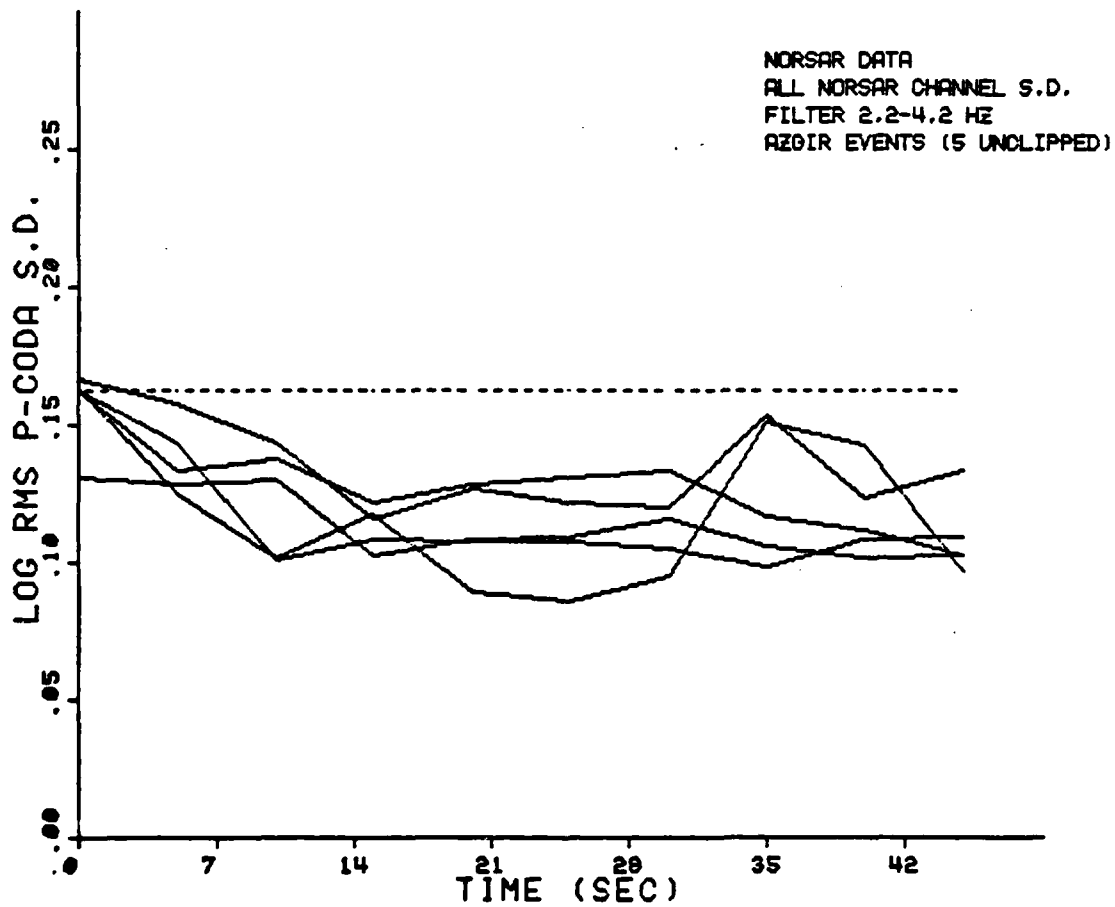


Figure 18. Same as Figure 17 except that 2.2 - 4.2 Hz filter has been applied. Note that coda standard deviation is below mean noise standard deviation.

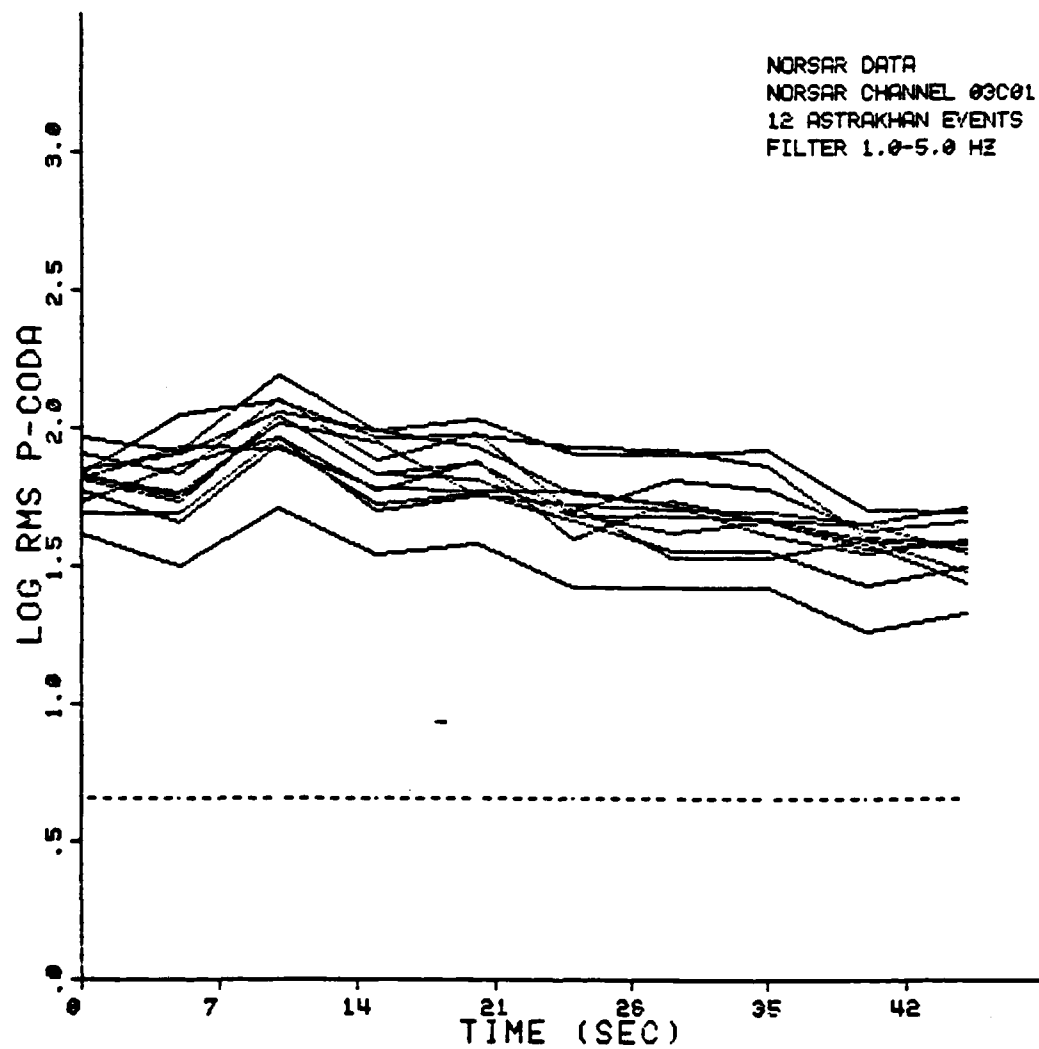


Figure 19. Log RMS amplitude envelopes for 12 unclipped Astrakhan events at the NORSAR 03C01 subarray element. Horizontal dashed line is mean noise level before P onset.

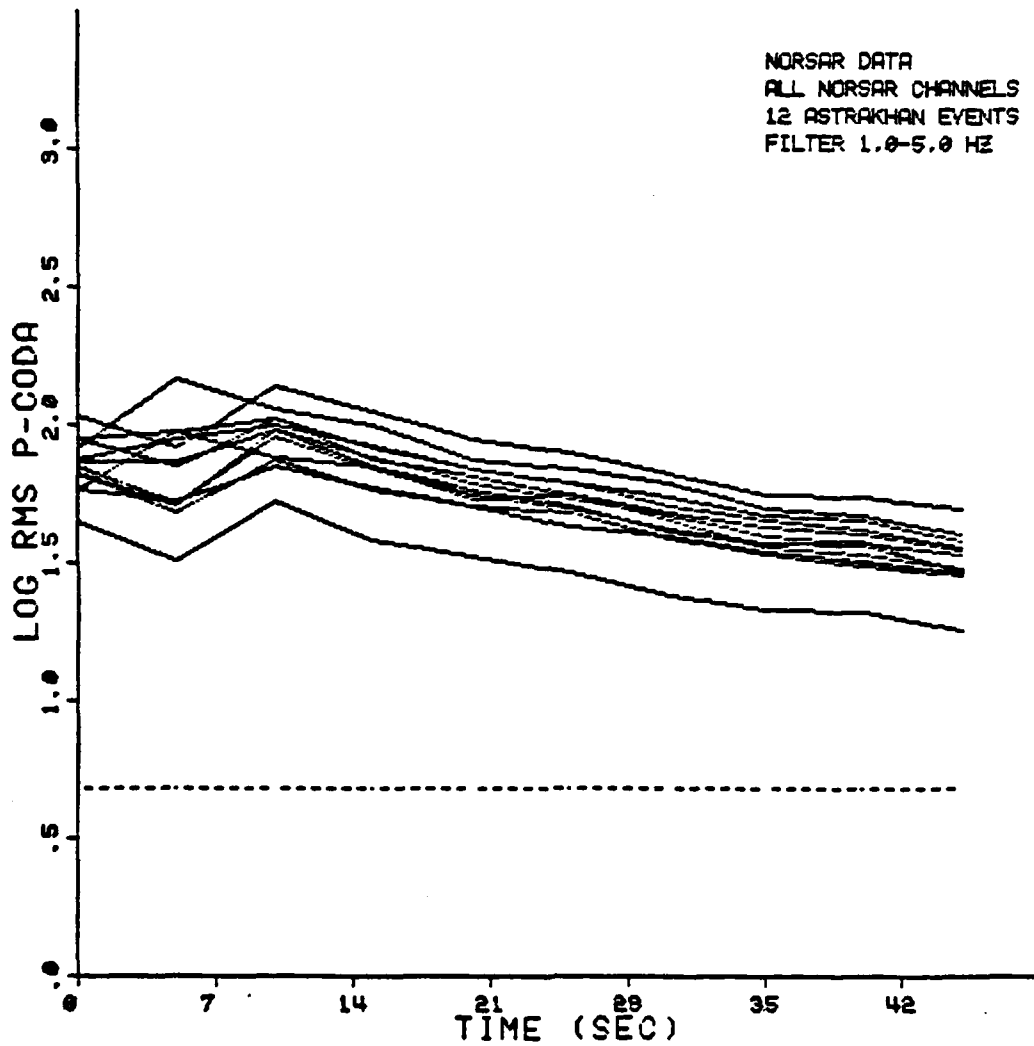


Figure 20. Same as Figure 19 except log RMS amplitudes are averaged over all available unclipped NOR SAR channels.

5.4 Comparing these coda envelopes with those for the Azgir events reveals that the former do not fall off as fast as the latter. Moreover, the Astrakhan events exhibit more frequent fluctuations with time into the coda on the single channel than do the Azgir events although these fluctuations are considerably smoothed out by averaging over several channels.

Figure 21 shows the standard deviations in log-RMS amplitudes in the early parts of the P codas for these events. We attribute the large jump in standard deviation at about 10 to 12 seconds into the coda to the same second-arrival P phase as observed in the Azgir events except delayed in time because Astrakhan is about one degree farther from NORSAR than Azgir. However, the Astrakhan standard deviations exhibit considerably more variability with time than the standard deviations of the Azgir events. Also, for some of the events, the standard deviations remain quite high relative to the noise level.

We conclude that the differences in characteristics of the codas for Azgir and Astrakhan are due mainly to differences in the near-source structure. Astrakhan codas are more intense and variable than the Azgir codas. Since these regions are so close together, the path and receiver scattering effects should be nearly the same which leaves only source differences as the most likely explanation for the observed differences in coda properties. These quantitative results agree with the qualitative comparison discussed earlier of the Azgir and Astrakhan event codas in Figure 1. In order to verify the conclusion that Astrakhan

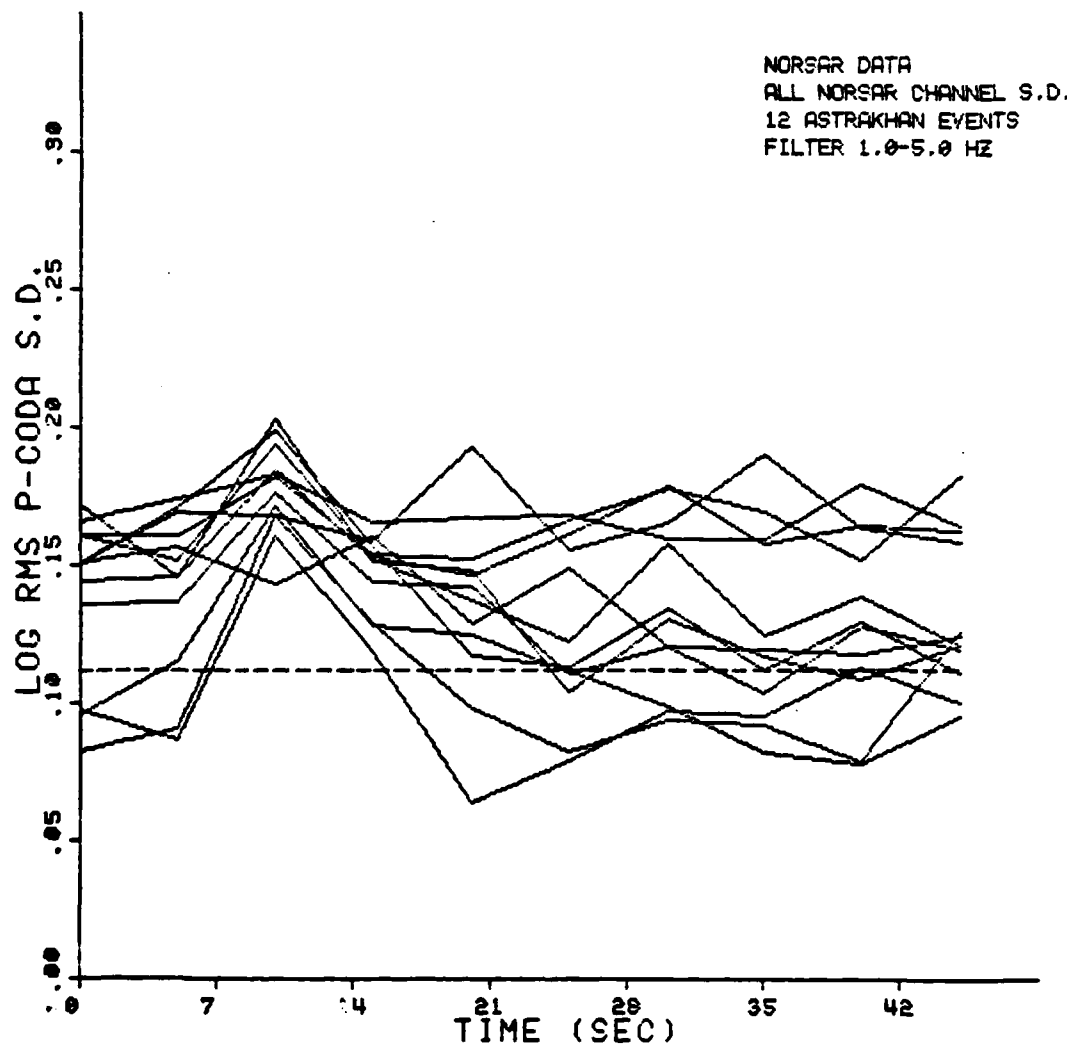


Figure 21. Standard deviations in the log RMS amplitudes across all unclipped NORSAR channels.

is more complex than Azgir, more geological data for these two regions needs to be examined.

3.0 ORIGIN OF CODAS FROM EURASIAN EVENTS

3.1 INTRODUCTION

In the last section, we reviewed various scattering mechanisms which have been proposed as causes of P-coda waves. In this section, we discuss those mechanisms or combination of mechanisms which may be responsible for generating P-coda waves from explosions in Russia. We will also consider much longer codas, including Lg and Lg-coda phases, than we did in Section 2.0. The main focus of this discussion will be on the Semipalatinsk events although we will briefly compare the long-term coda characteristics of Semipalatinsk and north Caspian Sea explosions.

3.2 LONG-CODAS FROM EURASIAN EXPLOSIONS

Figure 22 shows about 19 minutes of P and coda for three Semipalatinsk explosions recorded at NORSAR. Although NORSAR is about 38 degrees away from Semipalatinsk, Lg can be clearly observed as indicated on each of the traces although the Lg onsets are emergent and would be difficult to time accurately. In fact, in Ringdal's (1983) study of Lg, his 'Lg magnitude' is an integrated log-RMS amplitude measurement made on a 2-minute time window starting 40 seconds ahead of the expected Lg arrival time. Thus, these measurements are actually Lg and Lg-coda magnitudes rather than distinct Lg-phase measurements.

Figure 23 shows the log-RMS amplitude envelopes of about 16 minutes of P and coda for three Semipalatinsk

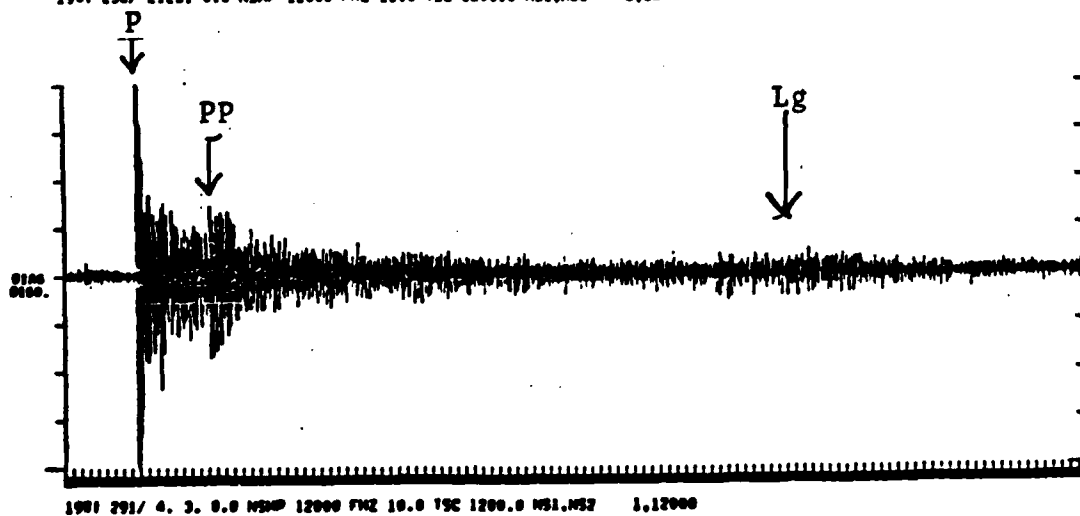
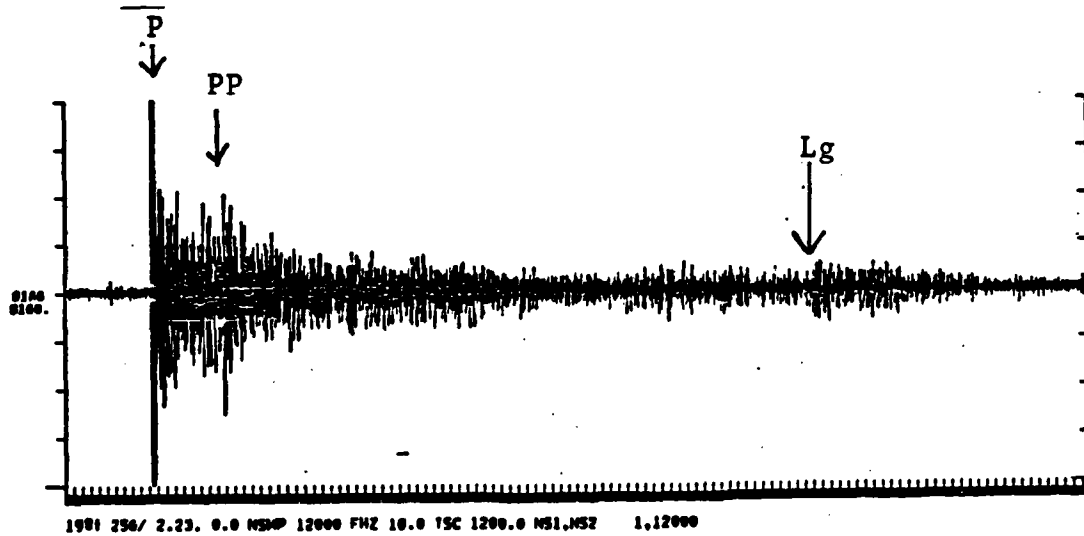
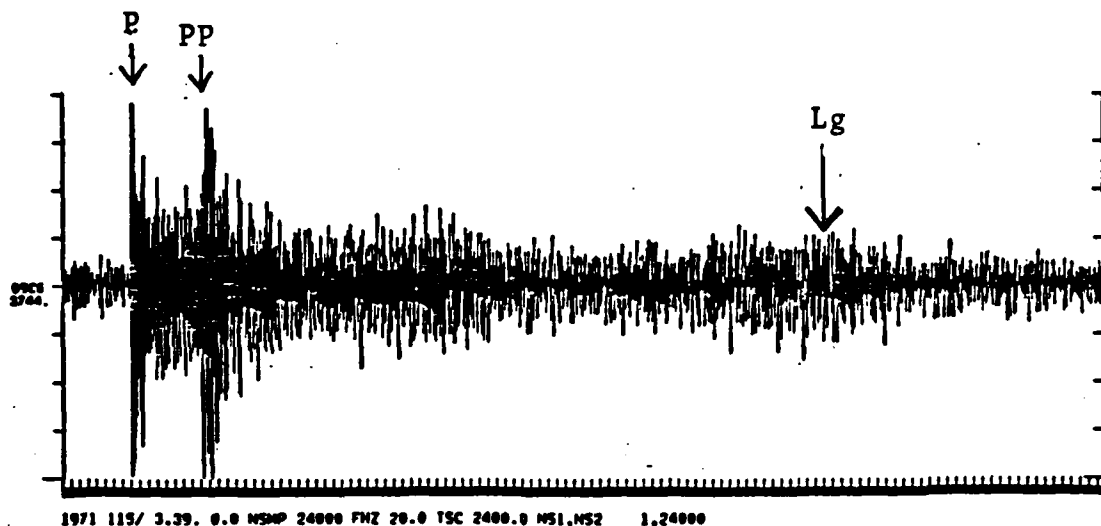


Figure 22. 3 Semipalatinsk explosions recorded at NORSAR.

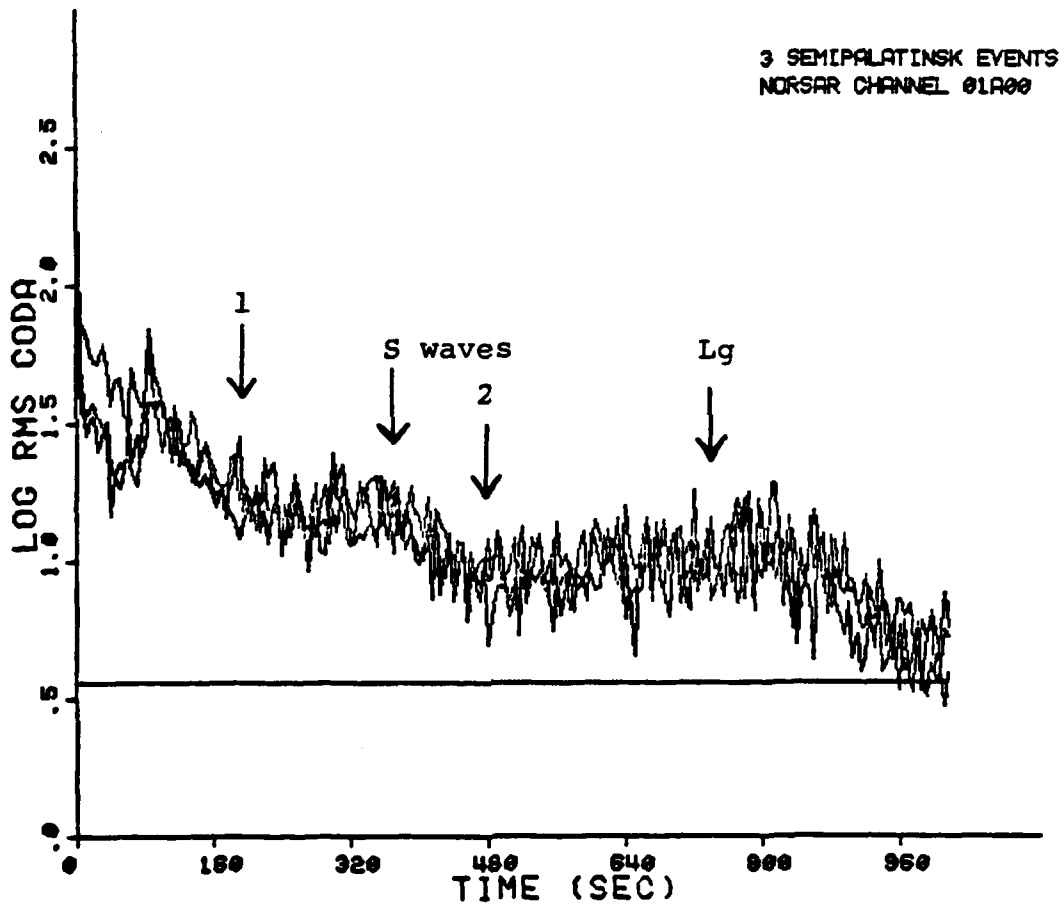


Figure 23. Log RMS amplitude levels for three presumed Semipalantinsk explosions recorded at channel 01A01 at NORSAR. The horizontal line designates the average noise background ahead of the P onset.

events as recorded on the 01A01 channel at NORSAR. Baumgardt (1983) has pointed out that Semipalatinsk coda shapes are very distinct from those of U. S. explosions at greater distances (greater than 60°) from NORSAR than Semipalatinsk. Instead of falling off exponentially with time, as observed in the U. S. explosions, the Semipalatinsk event codas pass through two steps, where the coda level flattens with time, before the Lg energy arrives. These two flat parts are indicated by the arrows numbered 1 and 2 in Figure 23. The increase in coda energy at the expected arrival time of Lg is also evident in Figure 23.

We argue that these flat parts of the coda reflect the arrival of seismic energy bursts caused by regional and/or scattered phases. The energy corresponding to burst number 1 in Figure 23 starts at about 200 seconds after P and burst number 2 is at about 480 seconds after P. Neither of these phases appear to correspond to shear waves, which are expected to arrive at about 353 seconds after P.

Contrast the Semipalatinsk codas with the coda of one of the Astrakhan events, shown in Figure 24. The log-RMS amplitude envelope for this event on channel 01A01 is shown in Figure 25. On these two plots, there appears to be no Lg phase in contrast to the clear Lg waves that can be observed at NORSAR for the Semipalatinsk explosions. Piwinskii and Springer (1978) also observed erratic Lg propagation across the southern portions of the Caspian Sea. Piwinskii (1981) argues that the reason for the poor Lg propagation across this region lies in the fact that the crustal structure of the Pri-Caspian Depression, as reported in the Russian geophysical literature, lacks a "granitic" upper-crustal

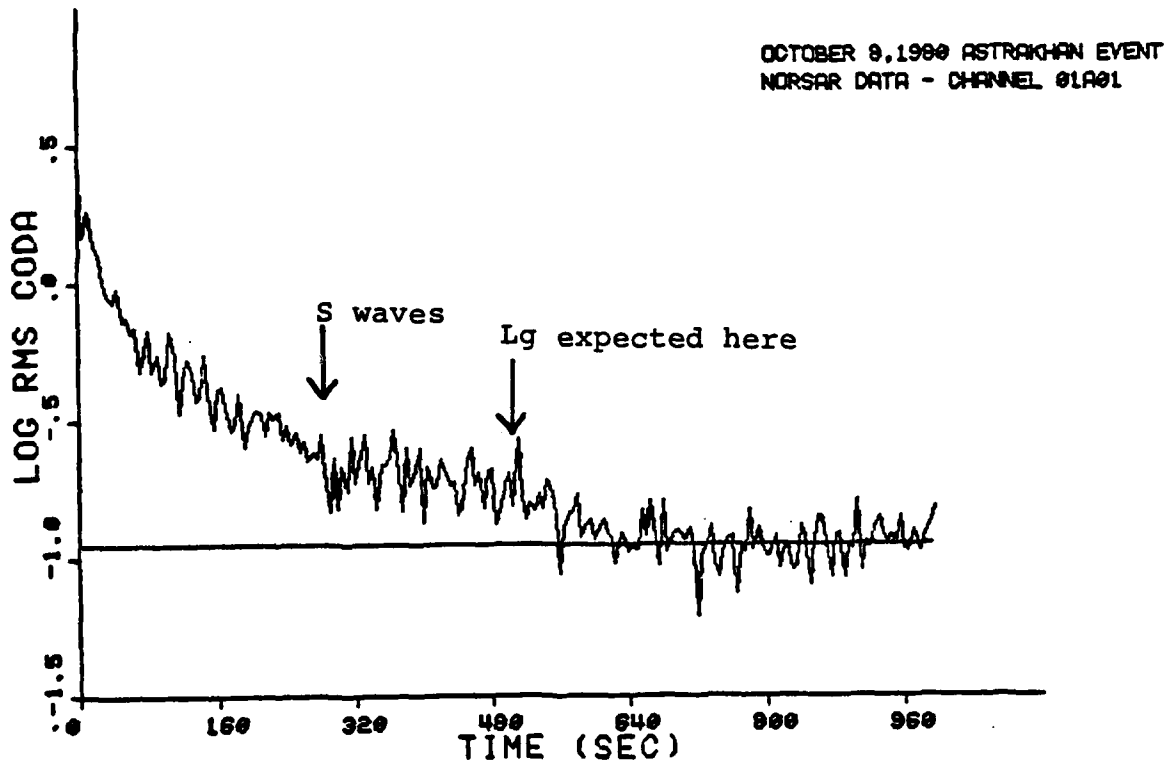


Figure 25. Log RMS amplitude envelopes for 16 minutes of P and coda for the 8 October 1980 Astrakhan event. Note that no strong Lg is apparent. Horizontal line denotes background noise level.

waveguide. The apparent flattening and increased variability of the coda at about 280 seconds after P may be due to the arrival of shear waves, as indicated in Figure 25. Aside from this, however, this coda exhibits the exponential falloff with time as observed in the case of the U. S. events recorded at NORSAR.

For the purposes of discussion, we identify two parts of the P coda at NORSAR for the Semipalatinsk events: PP precursor coda, between the P wave and the PP wave, which arrives about 100 seconds after P, and the Lg precursor coda, which includes all the coda from about 160 seconds after P to the Lg arrival time. In the remainder of this section, we argue that different scattering mechanisms dominate in generating coda waves in these two parts of the coda; body-wave scattering in the source, path, and receiver regions and Lg scattering along the path between source and receiver. We present these ideas as working hypotheses and present some preliminary evidence which support them. We will also discuss their significance with regard to using coda measurements for source characterization and yield estimation.

3.3 PP-PRECURSOR CODA WAVES

We have already discussed at some length the characteristics of PP-precursor coda waves in Section 2.0. The two key results of that study were, first, that the array-averaged log-RMS coda amplitudes, measured in 5 second windows for different events, decay more smoothly and consistently with time than single-channel measurements and, second, that the standard deviations across NORSAR of log

RMS amplitudes are comparable to those of random noise. Both of these observations support the contention that local scattering near the sensors at NORSAR contributes to PP-precursor coda. Local scattering would randomize the coda resulting in the coda perturbations observed in the single-channel coda-envelope plots and causing the coda standard deviations to resemble those of random noise.

Scattering in the source region undoubtedly also contributes to the PP-precursor coda since there is still a residual coda level remaining after averaging over all channels, as is evident in Figure 6. However, as was argued in Section 2.2, the relative contribution of source and receiver scattering to the coda is determined by the relative geologic complexity of source and receiver regions.

Greenfield (1971), Gupta (1983), and Gupta et al (1984) have made a strong case for the importance of fundamental-mode scattering in the source region as a mechanism for generating P-coda waves from explosions at Novaya Zemlya and at NTS. Moreover, Gupta (1983) and Gupta et al (1984) have suggested that coda waves may be used for characterizing different source regions as well as for estimating yields.

The results of our study of the north-Caspian-Sea explosions definitely support the idea of using codas to characterize source regions. We observe significant differences between the characteristics of Azgir and Astrakhan codas which we attribute to differences in the complexity of the source regions. We now consider the question of how important fundamental-mode surface-wave

scattering at Semipalatinsk is in producing P-coda waves at NORSAR.

Gupta (1983) has pointed out that null patterns, produced by P-PP interference, do not persist throughout the codas of NTS explosions recorded at NORSAR. This observation would favor the predominance of Rayleigh-to-P or Lg-to-P scattering from topographic inhomogeneities for generating the P coda. However, Baumgardt (1981) has observed persistent null patterns for about 40 seconds into the coda in sonograms of Semipalatinsk explosions recorded at the SDCS station RKON. Figure 26 shows a sonogram for part of the PP-precursor coda recorded at the 03B06 instrument at NORSAR for a Degelen event. Spectral null patterns appear to persist at least 30 seconds into the P coda and perhaps longer. However, we do not observe strong null patterns at all NORSAR channels for this event. The reason for this might be that near-receiver scattered waves may distort or mask the spectral nulls. An explanation for the fact that null patterns are observed for Semipalatinsk but not NTS suggests that NTS may have more surface relief, i.e., basins and ranges for Rayleigh-to-P scattering than does Semipalatinsk. This illustrates how differences in the observed characteristics of P codas can reveal insights into differences in the structure and topography of different source regions.

Figure 27 compares the magnitude residuals, with respect to the array mean, for P and coda measured on the 22 subarray centers and for the 4/25/71 Degelen event. If the coda is produced by P-wave scattering in the source region, these residuals should be positively correlated. Although

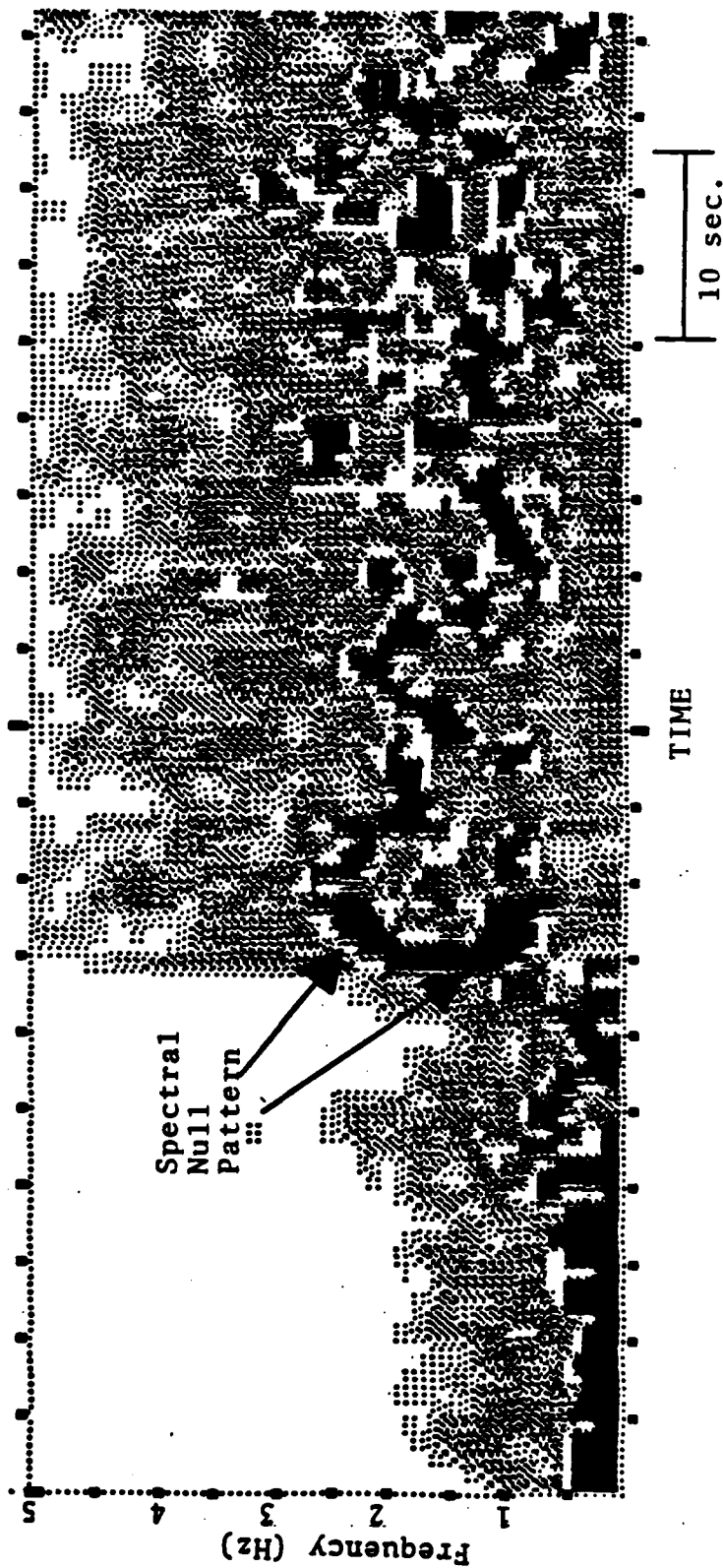


Figure 26. Sonogram of the Degelen explosion of 4/25/71 recorded on the 03B06 instrument at NORSAR. The black areas, bordered by white areas, are the high power (0-3dB down) parts of the spectra. Note the two persistent peaks between which is a null, which lasts for about 30 seconds into the coda.

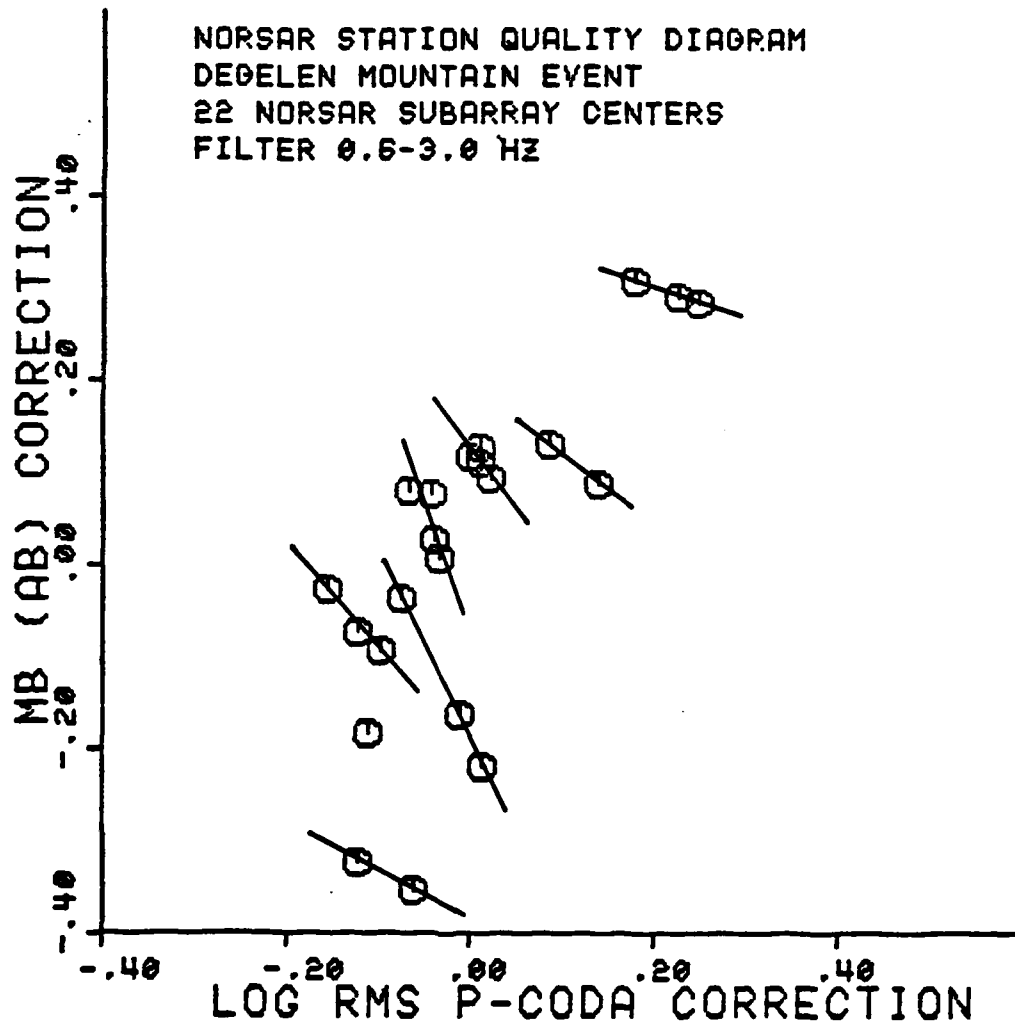


Figure 27. Plot of the P and coda magnitude residuals, with respect to the mean, measured at the 22 NORSAR subarray centers for the April 25, 1971 Degelen event.

the P- and coda-magnitude residuals are approximately correlated, there is a great deal of scatter in the data. In fact, the points are grouped together in linear trends with negative slopes, as shown by the lines drawn through them in Figure 27. We argue that the gross positive correlation between the groups of points in Figure 27 reflects source and receiver scattering and focusing-defocusing effects beneath NORSAR. However, the negative correlation between P and coda residuals within each group of points results from local scattering beneath the individual receivers. P and coda waves which 'see' the same kind of focusing effects are scattered differently, and the inverse slopes reflect the effect of scattering attenuation; i.e., the greater the scattering, the greater the coda magnitude and the smaller the P-wave magnitude.

Thus, we suggest that P-wave scattering and focusing and defocusing beneath NORSAR are the predominant mechanisms which modulate P and coda levels around the array. This does not rule out near-source scattering as also contributing to the overall base coda level although we would expect this contribution to be approximately the same at each of the NORSAR sensors.

In order to investigate the importance of surface-wave scattering to exciting P coda, we plot in Figure 28 the P-coda magnitudes from Table 1 and the Lg-coda magnitudes of Ringdal (1983), residualized with respect to the ISC or NEIS magnitudes, for the single 03C1 channel. Lg waves are believed to be a composite of higher-mode surface waves propagating through the continental crust. Fundamental mode surface waves at frequencies near 1 Hz are confined to the

very top 1 to 2 km of the crust have lower phase velocities and thus greater anelastic attenuation than higher modes, and therefore, do not propagate very far. Because they are confined to the top layers of the crust, fundamental modes may experience severe scattering from topographic heterogeneities which generate coda waves but because they don't propagate very far with high energy, they probably would not produce extended codas. Figure 28 appears to confirm this idea. Since we would expect that sources which generate large fundamental modes would also produce large higher-mode, or Lg, waves at frequencies near 1 Hz, we would expect a positive correlation between Lg and coda magnitudes if fundamental mode scattering produces the coda waves. No such correlation is evident in Figure 28.

Note, however, that the coda magnitudes used in Figure 28 average over 50 seconds of coda starting 5 seconds after P. Thus, we conclude that fundamental-mode scattering at Semipalatinsk does not significantly control long-term coda excitation at NORSAR. However, this mechanism may still produce short-term coda waves, say within 5 to 10 seconds after P. This idea is not addressed in this study. However, Gupta et al (1984) has found pulses within 5 seconds of P for NTS explosions whose spectral characteristics are consistent with their being produced by fundamental mode surface-wave scattering. A similar study needs to also be done for the Russian events.

We thus conclude overall that P-wave scattering in the source and receiver regions produces most of the PP-precursor coda waves. Also, it should be noted that asymmetric PP scattering from surface topography or in the

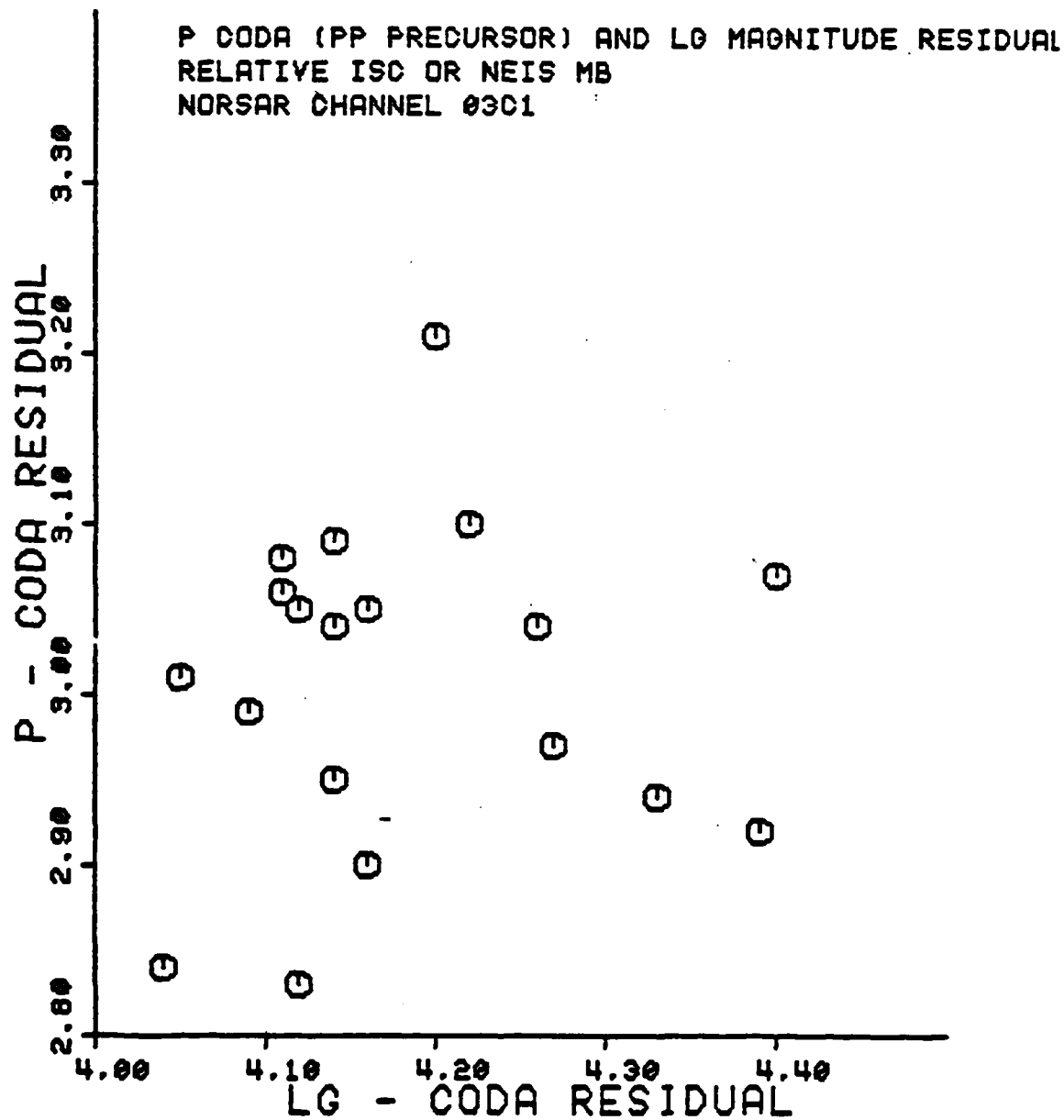


Figure 28. Residual, with respect to ISC or NEIS m_b , of the RMS coda magnitude versus the Lg residuals for channel 0301.

lithosphere along the path, as illustrated in Figure 2c, may also contribute to the coda. Finally, our analysis of Figure 27 suggests the intriguing possibility that the effects of focusing-defocusing and scattering attenuation on P waves may be separable by comparing P and coda magnitude residuals. Also, by doing this kind of comparison using a network of regional arrays, we might also be able to separate the effects of anelastic attenuation as well. If this can be done, then corrections can be devised, using P coda magnitudes, to correct for the effects of focusing-defocusing, scattering, and anelastic attenuation in biasing P-wave magnitudes.

3.4 LG PRECURSOR CODA WAVES AND LG SCATTERING

We now compare the characteristics of the PP-precursor coda and Lg precursor coda with the Lg and Lg-coda characteristics. To do this, we use the coda-measurement windows indicated in Figure 29. The PP-precursor window, or window 1 in Figure 29, begins 5 seconds after P and extends for 40 seconds into the coda. The Lg-precursor window, or window 2 in Figure 29, is the Lg and Lg-coda window which begins 760 seconds after P (8 seconds before expected Lg arrival time assuming a 3.5 km/sec group velocity) and extends for 200 seconds. Log-RMS amplitudes are measured in 5 second windows and then these estimates are averaged over the 3 windows.

Figures 30 and 31 compare the log-RMS amplitude measurements on the Lg and Lg coda (window 3) with those over the PP precursor coda (window 1) and the Lg precursor coda (window 2) recorded at NORSAR for the 4/25/71 Degelen

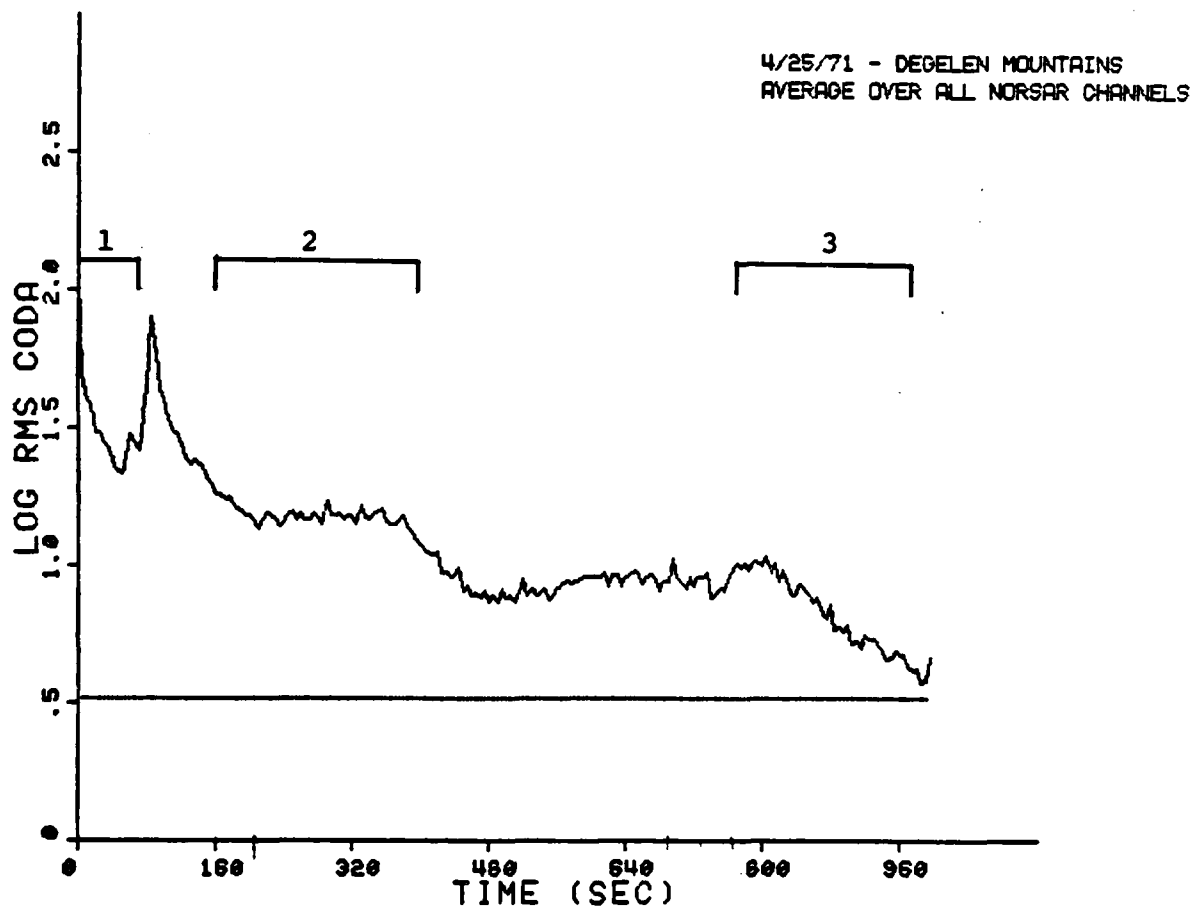


Figure 29. Coda measurement windows. Window 1 is P P-precursor window, window 2 is Lg precursor window, and window 3 denotes the Lg-coda measurement window. Horizontal line is the mean background noise level.

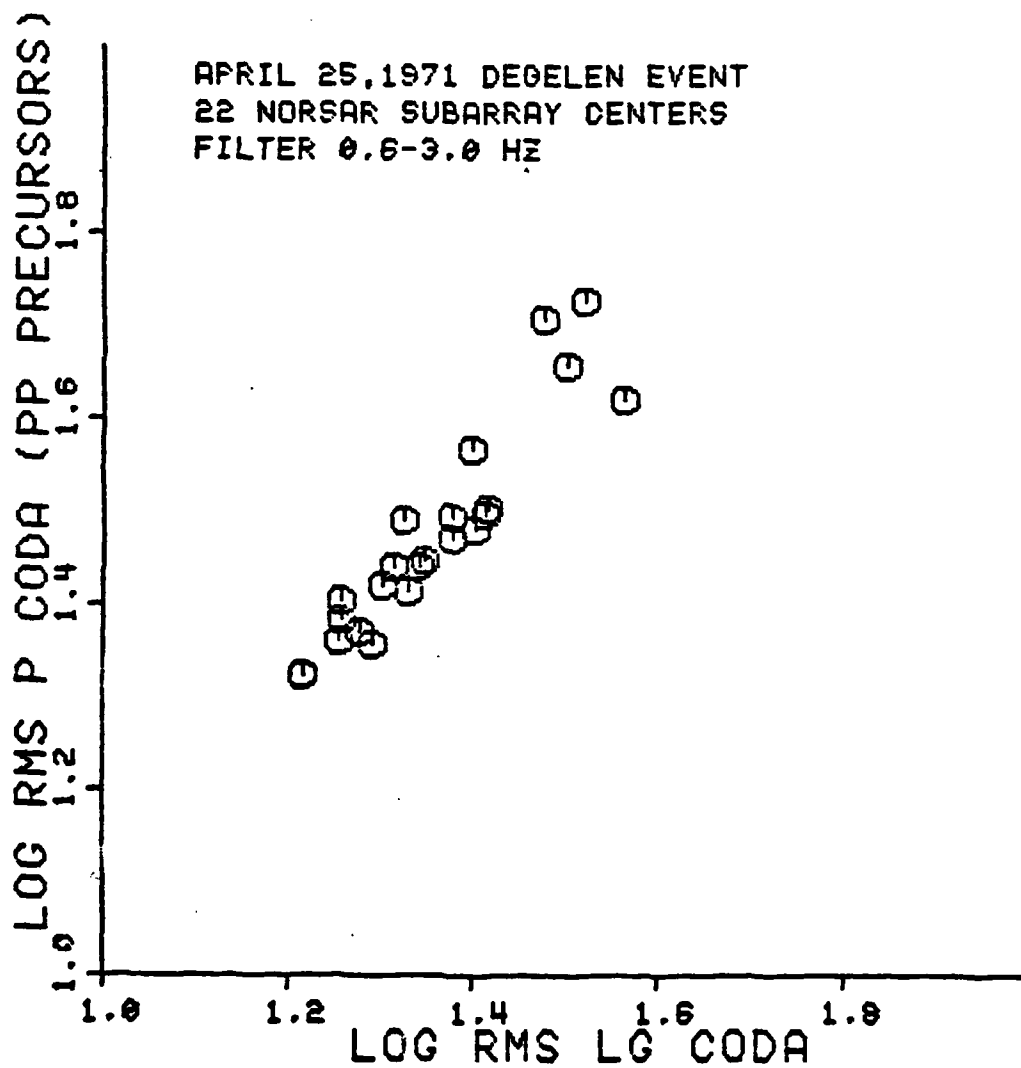


Figure 30. Plot of measurements of PP-precursor coda (window 1) against those of Lg and Lg-coda (window 3).

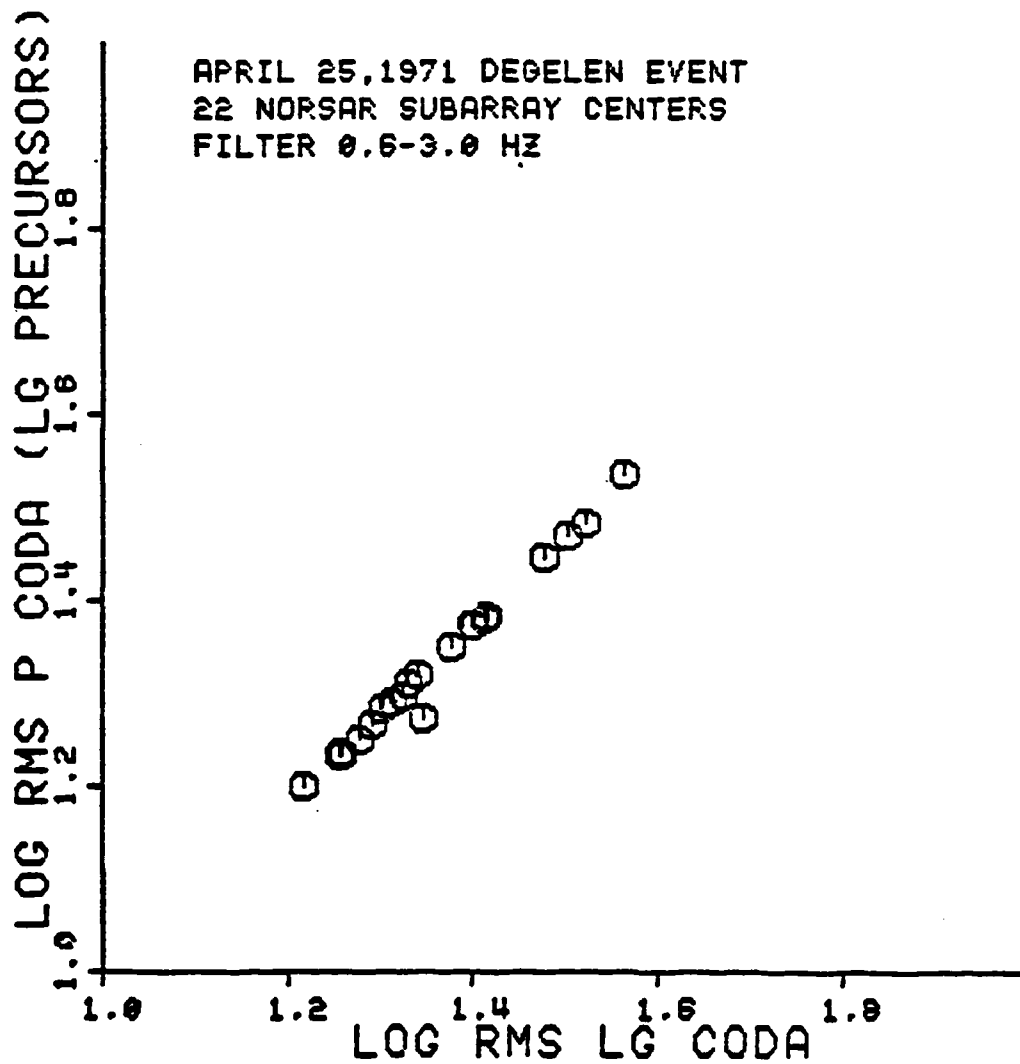


Figure 31. Plot of measurements of Lg-precursor coda (window 2) against those of Lg and Lg-coda (window 3).

event. Each point corresponds to a measurement made on one of the 22 NORSAR subarray center channels. A 0.6 to 3.0 Hz bandpass filter was applied to the data prior to making measurements.

It is evident from Figure 30 that PP-precursor coda and Lg and Lg-coda measurements are positively correlated although there is significant scatter in the data relative to a best-fitting line. However, Figure 31 shows that there is nearly a perfect correlation between the Lg precursor coda and the Lg and Lg-coda levels. Clearly, there appears to be a closer affinity between the phases in the first flat part of the coda and Lg than between the PP-precursor coda and Lg.

We suggest that the flat part of the coda in Figure 29 arises from Lg scattering to P at lateral heterogeneities in the crust along the Lg-propagation path from Semipalatinsk to NORSAR. Assuming that the flat part of the coda starts at about 200 seconds past P and stops at about 376 seconds past P, the Lg-scattered burst would have a duration of 176 seconds. The difference in arrival time between the Lg and the start and stop of the burst is 560 and 376 seconds, respectively. Assuming Lg is scattering to P during this period, the range of distances of the scattering points to NORSAR, using the regional travel-time curves for Eurasia in Gupta et al (1979) is about 19 to 30 degrees from NORSAR. Looking at a map of Eurasia (see Figure 32) we see that this distance range includes, from east to west, the Kazakh uplands, the northern extent of the Kazakh Steppes, and the southern portion of the Ural Mountains.

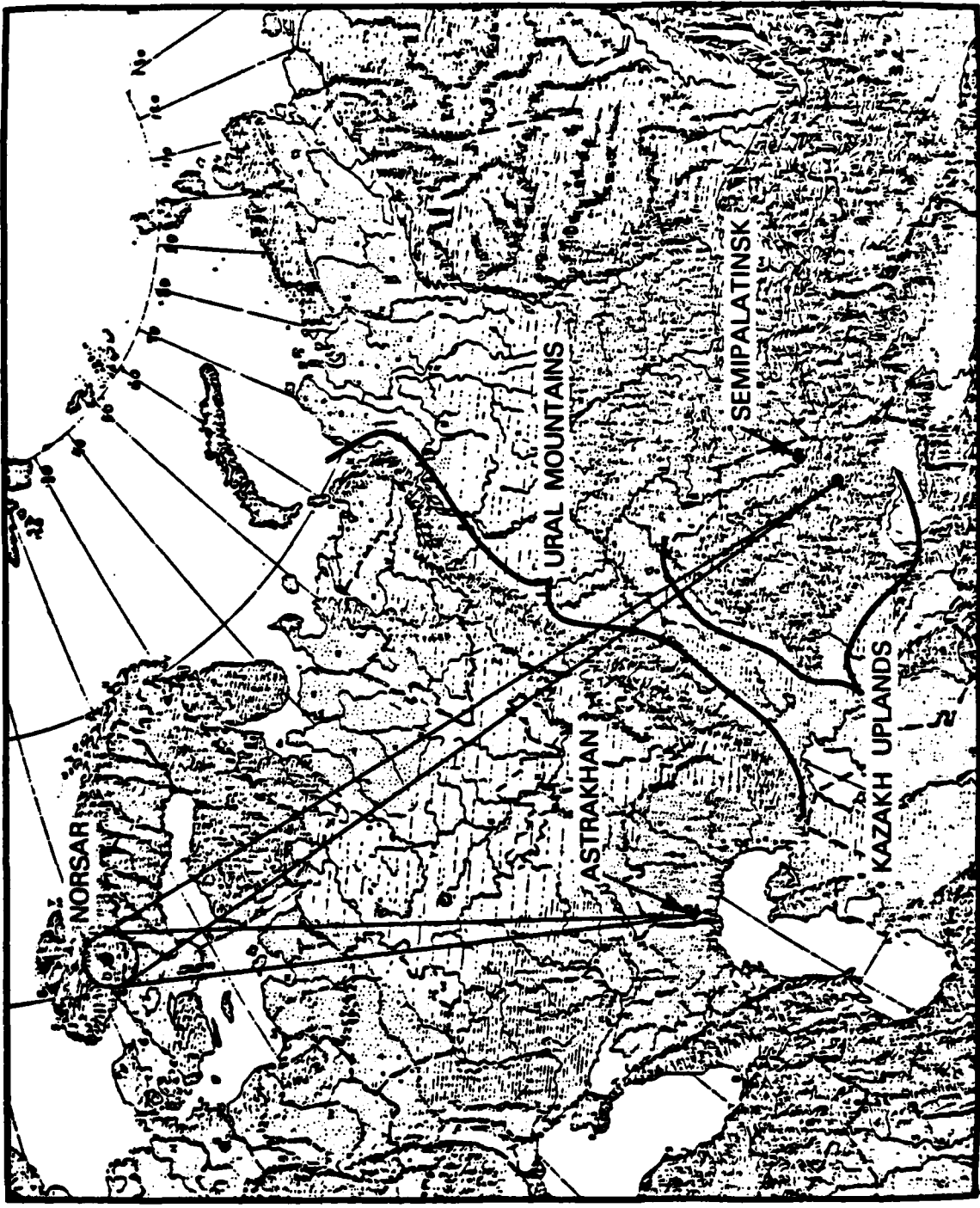


Figure 32. Physiographic map of Western Eurasia showing Lg propagation paths from Semipalatinsk and Astrakhan to NORSAR. Circle at NORSAR is approximate full-array aperture.

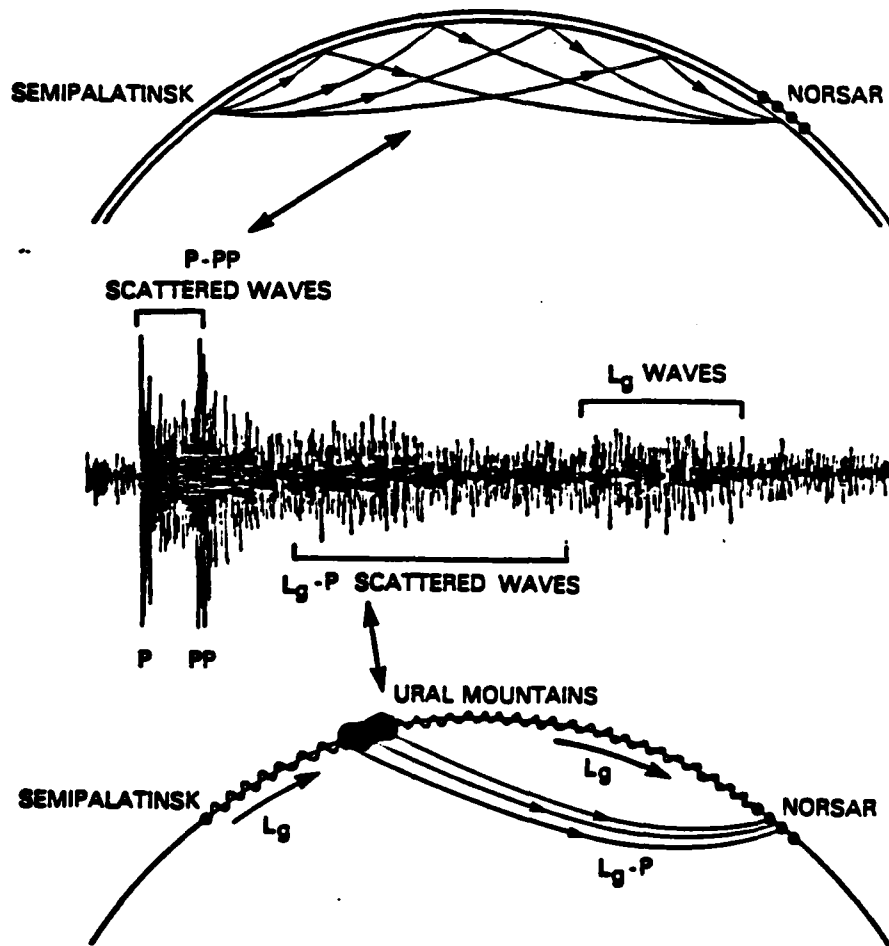
Figure 31 shows that there is a close correlation between variations around NORSAR in the log-RMS amplitude level in the scattered P waves arriving in the first flat part of the coda and those of the Lg waves. We suggest that these variations are caused by lateral variations in scattering from the Ural Mountains. The 100km aperture of the full NORSAR array used in the measurements in Figures 30 and 31 can receive Lg waves propagating across at least a 42 km segment of the north-south striking Ural Mountains at a distance of about 22 degrees from NORSAR (see Figure 32). This segment corresponds to several Lg wavelengths at 1 Hz. Also, lateral refraction and multipathing could cause Lg waves crossing the Urals over even a greater segment than 42 km to reach NORSAR. Thus, we expect a positive correlation between scattered Lg-to-P and Lg amplitudes and that the amplitude variations in Figure 31 are caused by lateral variations in the scattering of Lg in the 42 km or greater segment of the Ural Mountains.

Figure 32 shows the direct Lg propagation paths from Semipalatinsk and Astrakhan to NORSAR. Even though the two paths are both in the Baltic Shield, the Semipalatinsk-to-NORSAR path crosses many more topographic heterogeneities than the Astrakhan-to-NORSAR path. Thus, the differences in these two paths plus the observation that little or no Lg waves are produced by Astrakhan events explains the differences between the Semipalatinsk and Astrakhan coda envelope shapes.

3.5 SEMIPALATINSK EVENT CODAS - CONCLUSIONS

Figure 33 summarizes our conclusions regarding the origin of coda waves recorded at NORSAR for Semipalatinsk events. The portion of the coda between P and PP, or PP-precursor coda, is primarily caused by P and PP scattering. The rest of the coda between PP and Lg, or Lg-precursor coda, arises from Lg-to-P scattering from lateral topographic and geologic heterogeneities along the Lg propagation path between source and receiver and other regional phases, such as shear waves.

The close proximity of NORSAR to the Russian test sites should allow us to use coda magnitudes to estimate yields of events with body-wave magnitudes as low as 5.0 or less. From a signal-to-noise ratio standpoint, we might argue that the part of the coda between P and PP might be better for yield estimation than Lg since the PP-precursor coda level is about 0.75 magnitude units greater than the Lg level (Figure 29). However, our comparison of P-coda and Lg measurements in Section 2.0 suggests that Lg magnitudes may be more stable than PP-precursor coda magnitudes for yield estimation. Since there is such a close correlation between later, Lg-precursor coda magnitudes and Lg and because the first flat part of the coda is about 0.1 to 0.2 magnitude units above the Lg level, coda magnitudes measured in window number 2 in Figure 29 may be more stable for yield estimation than either PP-precursor coda measurements or Lg and Lg-coda measurements.



P CODA GENERATION MECHANISMS FOR SEMIPALATINSK EXPLOSIONS RECORDED AT NORSAR

Figure 33. Schematic illustration of postulated model for P-coda wave excitation from Semipalatinsk.

4.0 CONCLUSIONS AND RECOMMENDATIONS

4.1 CONCLUSIONS

The following conclusions were reached regarding the measurements on codas recorded at NORSAR for presumed Russian explosions.

- (i) NORSAR P-coda magnitudes for Semipalatinsk events vary across the array by about 0.1 magnitude units as compared with about 0.2 to 0.3 units for P-wave magnitudes. Also, array-averaged estimates of coda magnitude varied more smoothly with time into the coda than single-channel estimates. The same result was obtained for Azgir-Astrakhan events. These results suggest that local subarray scattering causes random perturbations in coda levels which are smoothed out by the averaging process.
- (ii) We find that NORSAR P-coda magnitudes, like the Lg measurements of Ringdal (1983), are more consistent with network averaged P-wave magnitudes than NORSAR single-channel magnitudes. There is some indication that Lg measurements may be slightly better than P-coda measurements in terms of reducing scatter and bias.
- (iii) The differences in characteristics of the codas for Azgir and Astrakhan are due mainly to differences in the near-source structure. Astrakhan codas are more intense and variable

than the Azgir codas. Since these regions are so close together, the path and receiver scattering effects should be nearly the same, which leaves only source differences as the most likely explanation for the observed differences in coda properties. Thus, we conclude that the Astrakhan region is more complex geologically than the Azgir region in terms of the effects of geologic structures on seismic wave propagation out of this source region. This conclusion is consistent with the fact that Azgir is closer to the center of the Pri-Caspian salt basin, where the geologic structure may be more laterally uniform, than the Astrakhan region.

- (iv) P-wave scattering in the source and receiver regions produces most of the coda energy between P and PP for Semipalatinsk events recorded at NORSAR. Comparison of coda measurements in this part of the coda and Lg and Lg-coda measurements indicate that fundamental and higher-mode scattering in the Semipalatinsk source region is less important than body-wave scattering in producing long-term coda between P and PP.
- (v) The coda between PP and Lg, or the Lg precursor coda, arises from Lg-to-P scattering and other regional phases, such as shear waves. The time between the energy burst in the coda and Lg is consistent with the burst being P waves produced by Lg-wave scattering in the vicinity of the southern Ural Mountains.

- (vi) Since there is such a close correlation between later Lg-precursor coda magnitudes and Lg and because the first flat part of the coda is about 0.1 to 0.2 magnitude units above the Lg level, coda magnitudes measured in window number 2 in Figure 29 may be more stable for yield estimation than either PP-precursor coda measurements or Lg and Lg-coda measurements.

4.2 RECOMMENDED FUTURE RESEARCH

Based on the results of this study, we recommend that the following studies be carried out:

- (i) Redo the comparison of P-coda and Lg magnitudes using a consistent measurement methodology.
- (ii) Investigate the effect of averaging-window length on the stability of coda and Lg magnitudes.
- (iii) Investigate the short-term coda (5 to 10 seconds after P) for Russian events to determine if fundamental-mode scattering is important in producing short-term coda phases.
- (iv) Compare coda magnitudes with fundamental-mode magnitudes on intermediate band seismograms, such as the mid-period RSTN band.
- (v) Detailed analytical studies of the surface-wave scattering mechanism need to be made. These studies need to address specifically how

fundamental- and higher-mode waves scatter to produce diving P waves. For example, can topographic expression scatter Lg waves as effectively as fundamental modes or do Lg waves scatter off of deeper seated structures, such as vertical impedance contrasts produced by deeply penetrating faults? Is Lg scattering more effective at producing long-term coda than fundamental-mode surface waves?

- (vi) Compare coda measurements in the flat part of the coda, which may be caused by Lg to P scattering, with Lg measurements for several events to see if they are as correlated as were the multichannel measurements for a single event in Figure 31. Measure the slowness and azimuths of the coda phases to see if they are consistent with P phases arriving from the Ural Mountains.
- (vii) Examine more diagrams like Figure 27, which we call a station-quality diagram. Such diagrams may be useful for studying the effects of focusing and defocusing and scattering attenuation on P-wave magnitudes.
- (viii) Investigate whether or not coda magnitudes measured in the flat part of the coda are more stable than those measured in the coda between P and PP.

ACKNOWLEDGEMENTS

The author wishes to gratefully acknowledge Dr. Frode Ringdal of NORSAR, Professor Kei Aki, Mr. Rushan Wu, and Mr. Robert Nowack of MIT, and Dr. Indira Gupta of Teledyne Geotech for some useful discussions. Dr. Frode Ringdal also provided the NORSAR data used in this study. Mr. Steve Newman and Mr. Mike Sullivan provided computer programming support.

REFERENCES

- Aki, K., Analysis of the Seismic Coda of Local Earthquakes as Scattered Waves, J. Geophys. Res., 74, pp. 615-631, 1969.
- Aki, K., Scattering and Attenuation, Bull. Seism. Soc. Am., 72, pp. 319-330, 1982.
- Aki, K. and B. Chouet, Origin of Coda Waves: Source, Attenuation, and Scattering Effects, J. Geophys. Res., 80, pp. 3322-3342, 1975.
- Alexander, S. S., The Use of Lg as an Independent Estimator of Yield and Practical Methods of Overcoming Effects of Non-Isotropic Source Excitation on Long-Period Surface Wave Signals, Presentation at the 5th Annual DARPA/AFOSR Symposium on Seismic Detection, Analysis, Discrimination, Yield Determination, Eastsound, Washington, 1983.
- Bache, T. C., W. J. Best, R. R. Blandford, G. V. Bulin, D. G. Harkrider, E. J. Herrin, A. Ryall, and M. J. Shore, A Technical Assessment of Seismic Yield Estimation, DARPA-NMR-81-02, Defense Advanced Research Projects Agency, Arlington, Virginia, 1981.
- Bache, T. C., Estimating the Yield of Underground Nuclear Explosions, Bull. Seism. Soc. Am., Vol. 72, pp. 131-168, 1982.
- Baumgardt, D. R., Seismic Body-Wave Study of Vertical and Lateral Heterogeneity in the Earth's Interior, Ph.D. Thesis, The Pennsylvania State University, University Park, Pennsylvania, 1981.
- Baumgardt, D. R., Teleseismic P-coda Stability and Coda Magnitude Yield Estimation, Semiannual Technical Report, SAS-TR-83-01, ENSCO, Inc., Springfield, Virginia, 1983.
- Bullitt, J. T. and V. F. Cormier, The Relative Performance of M_b and Alternative Measures of Elastic Energy in Estimating Source Size and Explosion Yield, Submitted to Bull. Seism. Soc. Am., 1983.

Chen, T. C., Relation Between the Excitation of Long- and Short-Period Surface Waves from Underground Nuclear Explosions at NTS, abstract in EOS, Transactions, American Geophysical Union, 62, p. 330, 1981.

Cleary, J. R., and D. W. King, and R. A. W. Haddon, P-Wave Scattering in the Earth's Crust and Upper Mantle, Geophys. J. R. Astr. Soc., 43, pp. 861-872, 1975.

Greenfield, R. J., Short-Period P-Wave Generation by Rayleigh-Wave Scattering at Novaya Zemlya, J. Geophys. Res., 76, pp. 7988-8002, 1971.

Gupta, I. N., B. W. Barker, J. A. Burnett, and Z. A. Der, A Study of Regional Phases from Earthquakes and Explosions in Western Russia, in Studies of Seismic Wave Characteristics at Regional Distances, Technical Report, AL-80-1, Teledyne Geotech, Alexandria, Virginia, 1979.

Gupta, I. N., Coda Magnitude, Presentation at the 5th Annual DARPA/AOSR Symposium on Seismic Detection, Analysis, Discrimination, Yield Determination, Eastsound, Washington, 1983.

Gupta, I. N., R. R. Blandford, R. A. Wagner, and J. A. Burnett, Use of P Coda for Explosion Medium and Improved Yield Determination, Abstract, Annual Meeting, Seismological Society of America, Anchorage, Alaska, 1984.

Hudson, J. A. Use of Stochastic Models in Seismology, Geophys. J. R. Astr. Soc., 69, pp. 649-657, 1982

Kedrovskiy, O. L., The application of contained nuclear explosions for creating underground reservoirs and testing their operation for the storage of gas condensate, Peaceful Nuclear Explosions IV, International Atomic Energy Agency, pp. 227-255, 1975.

Key, F. A., Signal-Generated Noise Recorded at the Eskdalemuir Seismometer Array Station, Bull. Seism. Soc. Am., 57, pp. 27-38, 1967.

King, D. W., R. A. W. Haddon, and E. S. Husebye, Precursors to PP, Phys. Earth Planet, Int., 10, pp. 103-127, 1975.

Mack, H., Nature of Short-Period P-Wave Signal Variations at LASA, J. Geophys. Res., 74, pp. 3161-3170, 1969.

Mitchell, B. J., Effect of Crustal Velocities and Q on the

Amplitudes of Lg at Short and Intermediate Periods, AFOSR Semi-Annual Report, 31 March 1983.

Nuttli, O. W., Seismic Wave Attenuation and Magnitude Relations for Eastern North America, J. Geophys. Res., 78, pp. 876-885, 1973.

Murphy, J. R. and T. J. Bennett, Interim Report on the Status of the Yield Estimation Evaluation Program, (NSC-TR-83-9, S³, La Jolla, California, 1983 (SECRET). ✓

Nordyke, M. D., A Review of Soviet Data on the Peaceful Uses of Nuclear Explosions, Rept. UCRL-5144, Lawrence Livermore National Laboratories, Livermore, California, 1973.

Nuttli, O. W., A Methodology for Obtaining Seismic Yield Estimates of Underground Explosions Using Short-Period Lg Waves, AFOSR Semiannual Report, 31 March 1983.

Nuttli, O. W., Illustration of Use of Coda Q Method of Obtaining Anelastic Attenuation Values for Paths from Salmon (Mississippi) and NTS Events, AFOSR Semiannual Report, 30 November 1983.

Osage, E. O. and B. J. Mitchell, Regional Variation of Q_p and its Frequency Dependence in the Crust of South America, FOSR Semiannual Report, 30 November 1983.

Piwinskii, A. J., and D. L. Springer, Propagation of Lg Waves Across Eastern Europe and Asia, Report UCRL-52494, Lawrence Livermore National Laboratory, Livermore, California, 1978.

Piwinskii, A. J., Deep Structure of the Earth's Crust and Upper Mantle in the USSR According to Geological, Geophysical, and Seismological Data: Dneiper-Donetsk and Pri-caspian Depressions, UCID-19203, Lawrence Livermore Laboratory, Livermore, California, 1981.

Ringdal, F., G. Young and D. Baumgardt, Study of Detection and Location Techniques for Seismic Events Near Azgir, USSR: I, NORSAR Detection and Location Results, (Technical Report No. 1, SAS-TR-82-01, ENSCO, Inc., Springfield, Virginia, 1983 (SECRET) ✓

Ringdal, F., Location of Regional Events using Travel Time Differentials between P Arrival Branches, NORSAR Semiannual Technical Summary, 1 October 1980-31 March 1981, 1981.

Ringdal, F., Magnitudes from P Coda and Lg Using NORSAR Data, NORSAR Semiannual Technical Summary, 1 October 1982-31 March 1983, 1983.

Roundout Associates, The Use of Intermediate and Long-Period Seismic Waves for Discrimination and Yield Estimation, Annual Technical Report No. 2, Roundout Associates, Inc., Stone Ridge, New York, 1981.

Wright, C. and K. J. Muirhead, Longitudinal Waves from Novaya Zemlya Nuclear Explosin of October 27, 1966, Recorded at the Warramunga Seismic Array, J. Geophys. Res., 74, pp. 2034-2047, 1969.